

Combination anti-HIV antibodies provide sustained virological suppression

<https://doi.org/10.1038/s41586-022-04797-9>

Received: 25 October 2021

Accepted: 25 April 2022

Published online: 01 June 2022

 Check for updates

Michael C. Sneller^{1,10}, Jana Blazkova^{1,10}, J. Shawn Justement¹, Victoria Shi¹, Brooke D. Kennedy¹, Kathleen Gittens², Jekaterina Tolstenko¹, Genevieve McCormack¹, Emily J. Whitehead¹, Rachel F. Schneck¹, Michael A. Proschan³, Erika Benko⁴, Colin Kovacs⁴, Cihan Oguz^{5,6}, Michael S. Seaman⁷, Marina Caskey⁸, Michel C. Nussenzweig^{8,9}, Anthony S. Fauci¹, Susan Moir^{1,10} & Tae-Wook Chun^{1,10}✉

Antiretroviral therapy is highly effective in suppressing human immunodeficiency virus (HIV)¹. However, eradication of the virus in individuals with HIV has not been possible to date². Given that HIV suppression requires life-long antiretroviral therapy, predominantly on a daily basis, there is a need to develop clinically effective alternatives that use long-acting antiviral agents to inhibit viral replication³. Here we report the results of a two-component clinical trial involving the passive transfer of two HIV-specific broadly neutralizing monoclonal antibodies, 3BNC117 and 10-1074. The first component was a randomized, double-blind, placebo-controlled trial that enrolled participants who initiated antiretroviral therapy during the acute/early phase of HIV infection. The second component was an open-label single-arm trial that enrolled individuals with viraemic control who were naive to antiretroviral therapy. Up to 8 infusions of 3BNC117 and 10-1074, administered over a period of 24 weeks, were well tolerated without any serious adverse events related to the infusions. Compared with the placebo, the combination broadly neutralizing monoclonal antibodies maintained complete suppression of plasma viraemia (for up to 43 weeks) after analytical treatment interruption, provided that no antibody-resistant HIV was detected at the baseline in the study participants. Similarly, potent HIV suppression was seen in the antiretroviral-therapy-naive study participants with viraemia carrying sensitive virus at the baseline. Our data demonstrate that combination therapy with broadly neutralizing monoclonal antibodies can provide long-term virological suppression without antiretroviral therapy in individuals with HIV, and our experience offers guidance for future clinical trials involving next-generation antibodies with long half-lives.

Modern antiretroviral therapy (ART) enables the near-complete suppression of plasma viraemia in most individuals with HIV¹. However, difficulties in adherence to a lifetime of medication, long-term side effects and the possibility for developing antiretroviral drug-resistant virus have prompted intense research aimed at developing new therapies to achieve sustained virological remission without the need for daily ART⁴. In this regard, considerable efforts have focused on eliminating the persistent HIV reservoir^{5,6}—one of the major impediments to viral eradication^{7–9}—in individuals with HIV receiving clinically effective ART¹⁰. However, despite decades of research, it is becoming increasingly clear that complete eradication of the persistent HIV reservoir in an individual with infection is not feasible using currently available approaches and therapies¹¹. In the absence of an effective vaccine against HIV and/

or therapeutic agents that can eradicate the persistent viral reservoir, long-term suppression of plasma viraemia by infrequent administration of long-acting antiretroviral drugs^{12–14} or broadly neutralizing monoclonal antibodies (bNAbs)^{15–18} against HIV remains the most realistic approach for achieving ART-free virological suppression. In this regard, passive transfer of single bNAbs in individuals with HIV in the context of analytical treatment interruption (ATI) has shown limited success in part due to the presence of pre-existing and/or emergent antibody-resistant virus^{19–22}. To mitigate this shortcoming, a combination approach involving the use of two bNAbs that bind to different regions of the HIV Env glycoprotein has led to promising results^{15,23}. One such study used two bNAbs—one targeting the CD4-binding site on the HIV Env spike (3BNC117) and the other targeting the V3 loop and

¹Laboratory of Immunoregulation, National Institute of Allergy and Infectious Diseases (NIAID), National Institutes of Health (NIH), Bethesda, MD, USA. ²Critical Care Medicine Department, Clinical Center, NIH, Bethesda, MD, USA. ³Biostatistics Research Branch, NIAID, NIH, Bethesda, MD, USA. ⁴Maple Leaf Medical Clinic, Toronto, Ontario, Canada. ⁵NIAID Collaborative Bioinformatics Resource, NIAID, NIH, Bethesda, MD, USA. ⁶Advanced Biomedical Computational Science, Frederick National Laboratory for Cancer Research, Frederick, MD, USA. ⁷Center for Virology and Vaccine Research, Beth Israel Deaconess Medical Center, Harvard Medical School, Boston, MA, USA. ⁸Laboratory of Molecular Immunology, The Rockefeller University, New York, NY, USA. ⁹Howard Hughes Medical Institute, The Rockefeller University, New York, NY, USA. ¹⁰These authors contributed equally: Michael C. Sneller, Jana Blazkova, Susan Moir, Tae-Wook Chun. ✉e-mail: twchun@nih.gov

surrounding glycans (10-1074)—demonstrated that three infusions over a period of 6 weeks significantly delayed plasma viral rebound in individuals with infection after ATI²³. Furthermore, previous studies have suggested that, besides their ability to neutralize HIV, certain bNABs could potentially mediate the clearance of persistent viral reservoirs and/or enhance host immunity against the virus^{24–27}. Accordingly, we conducted this study to further investigate the long-term effect of treatment with a combination of the bNABs 3BNC117 and 10-1074 on the suppression of plasma viraemia and the dynamics of persistent viral reservoirs and their effect on immune parameters/responses in individuals with HIV.

Study design and participants

Between September 2018 and January 2021, we conducted a phase 1 clinical trial to assess the safety, tolerability and efficacy of the combination of the bNABs 3BNC117 and 10-1074 in individuals with HIV. This trial comprised two components: (1) a randomized, double-blind, placebo-controlled study involving 14 participants in whom ART was initiated during the acute/early phase of infection and who subsequently underwent ATI shortly after receiving the first infusion of bNABs or placebo (group 1); and (2) an open-label study involving 5 individuals with viraemic control who were naive for ART and had baseline plasma viraemia of between 200–5,000 copies per ml (group 2) (Table 1, Extended Data Fig. 1 and Supplementary Table 1). The study participants were not prescreened for the sensitivity of their HIV to 3BNC117 and 10-1074 before enrolment (the study inclusion criteria are described in the Methods). The randomized controlled portion of the study had a planned enrolment of 30 study participants. However, the study was prematurely halted in March 2020 owing to the increased safety concerns associated with ATI in the setting of the COVID-19 pandemic.

The study participants in the antibody arm of group 1 and group 2 received 4–8 (median, 8) 3BNC117 (30 mg kg⁻¹) and 10-1074 (30 mg kg⁻¹) infusions—two in the first month and once monthly thereafter (Fig. 1a). The infusions of bNABs were well tolerated, with most adverse events being mild-to-moderate (grade 1 or 2) transient symptoms, including chills and/or fever (Supplementary Table 2). One study participant in group 1 (participant 01) experienced grade 1 fever and grade 2 rigors during the first 3BNC117 infusion and did not receive the first dose of 10-1074. Thus, this participant was effectively on antibody monotherapy for the first 2 weeks of the study. For subsequent infusions, participant 01 was premedicated with ibuprofen and completed the remaining study infusions of both antibodies with minimal (grade 1) or no reactions. No participant discontinued study medications due to antibody-related adverse events. There was no grade 3 or higher adverse event, including serious adverse events that were judged to be possibly, probably or definitely related to the study drugs. The baseline median CD4⁺ T cell counts for the antibody and the placebo arm of group 1 were 799 and 612 cells per µl, respectively (Table 1). The baseline median CD4⁺ T cell count of group 2 was 640 cells per µl (Table 1).

Effect of bNABs on virological parameters

Three days after receiving the first infusion of 3BNC117 and 10-1074 or placebo, the study participants in group 1 underwent ATI and plasma viraemia and CD4⁺ T cell counts were measured every 2 weeks (Fig. 1a). For group 1, the protocol-predefined virological end point was the difference between the bNAB and placebo arms in the number of study participants who experienced plasma viral rebound and met the criteria to restart ART before study week 28. As shown in Fig. 1b, c, 6 out of the 7 study participants in the placebo arm experienced plasma viral rebound and met the criteria to restart ART before study week 28 compared with none of the 7 participants in the treatment arm. The median duration off ART was 39.6 weeks (range, 9.9–49.6 weeks) and 9.4 weeks (range, 5.3–26 weeks) for the group 1 bNAB and placebo

Table 1 | Baseline characteristics of the study participants.

Characteristic	Group 1		Group 2
	Antibody arm (n=7)	Placebo arm (n=7)	n=5
Sex, number (%)			
Male	7 (100)	7 (100)	5 (100)
Median age (range) (years)	40 (27–57)	34 (29–56)	44 (35–52)
Race or ethnic group, number (%)			
African American	1 (14.3)	0	1 (20)
Caucasian	4 (57.1)	5 (71.4)	3 (60)
Hispanic	1 (14.3)	1 (14.3)	0
Asian	1 (14.3)	1 (14.3)	0
Mixed	0	0	1 (20)
Antiretroviral regimen, number (%)			
NRTI	7 (100)	7 (100)	–
NNRTI	1 (14.3)	0	–
PI/INSTI	1 (14.3)	0	–
INSTI	6 (85.7)	7 (100)	–
PK	2 (28.6)	2 (28.6)	–
Inclusion criteria met ^a , number (%)			
Acute infection	5 (71.4)	2 (28.6)	–
Early infection	2 (28.6)	5 (71.4)	–
Reported seroconversion illness, number (%)	5 (71.4)	4 (57.1)	–
Median time between HIV diagnosis and start of ART (days) (range)	22 (0–50)	38 (9–76)	–
Median duration of suppressive ART at study entry ^b (years) (range)	3.7 (2.6–12.6)	2.9 (1.6–6.6)	–
Median CD4 ⁺ T cell count (cells per mm ³ at study entry) (range)	799 (543–1,177)	612 (426–832)	640 (527–1,011)

^aSee Methods for the acute and early infection inclusion criteria.

^bIndicates the duration of uninterrupted suppression of plasma viraemia.

INSTI, integrase strand transfer inhibitor; NNRTI, non-nucleoside reverse transcriptase inhibitor; NRTI, nucleoside reverse transcriptase inhibitor; PI, protease inhibitor; PK, pharmacokinetic enhancer.

participants, respectively ($P = 0.001$; Fig. 1c (left)). Notably, participant 11, in the placebo arm, who did not meet criteria to restart ART, deviated from the protocol and surreptitiously resumed ART at study week 12 owing to concerns about rising plasma viraemia. Participant 14, in the bNAB arm, reinitiated ART before meeting the restart criteria due to concerns associated with the COVID-19 pandemic. Thus, the data from these participants were censored for end-point analysis.

In an additional post hoc analysis, 5 out of the 7 study participants in the bNAB arm of group 1 maintained suppression of plasma viraemia (<40 copies per ml), whereas all of the study participants in the placebo arm of group 1 experienced plasma viral rebound within the first 8 weeks of ATI. The median duration of plasma viraemia suppression at <200 copies per ml in group 1 was 33.4 weeks (range, 7.4–43.3 weeks) and 3.4 weeks (range, 1.9–7.9 weeks) in the bNAB and placebo arms, respectively ($P = 0.002$; Fig. 1c (right)). Notably, two group 1 bNAB study participants (01 and 14), whose plasma viraemia rebounded by more than 200 copies per ml within 8 weeks into ATI, carried bNAB-resistant, replication-competent HIV in their CD4⁺ T cells at the baseline (Fig. 2a).

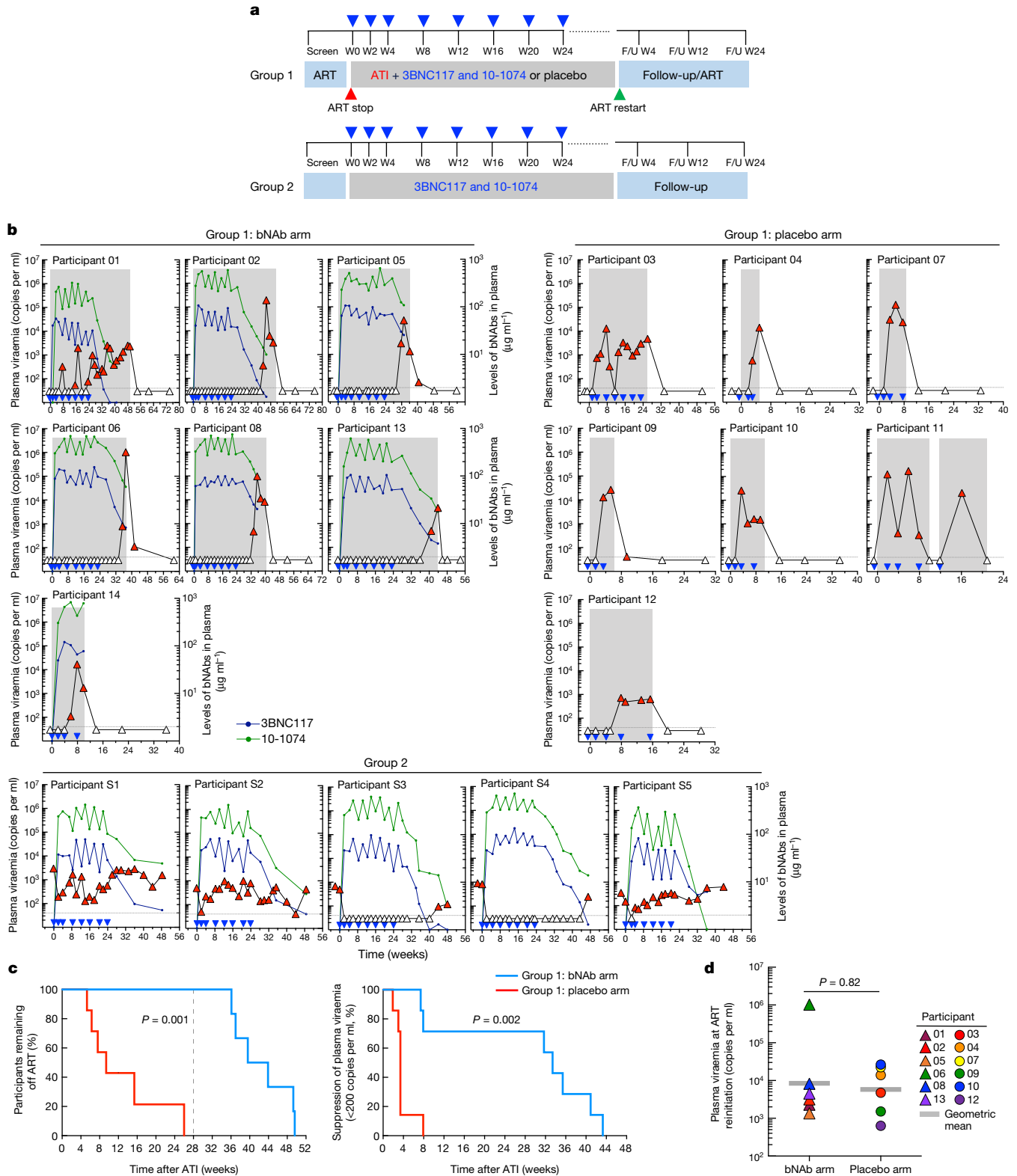


Fig. 1 | See next page for caption.

The median duration of suppression of plasma viraemia at below 200 copies per ml for the participants with sensitive virus was 35.4 weeks (range, 31.7–43.3 weeks). There was no difference in the level of plasma viraemia before reinitiation of ART between the bNAb and placebo arms in the group 1 study participants ($P = 0.82$; Fig. 1d), suggesting that bNAb-mediated virological suppression may not necessarily alter the kinetics of plasma viral rebound after clearance of the antibodies

in vivo. In group 2, 2 out of the 5 study participants whose baseline infectious HIV was sensitive to both antibodies maintained complete suppression of plasma viraemia for an average of 41.7 weeks (Figs. 1b and 2a). Taken together, these results demonstrate that the combination therapy with 3BNC117 and 10-1074 is highly effective in suppressing HIV in the absence of ART for extended periods, provided that antibody-resistant virus is not present at the baseline.

Fig. 1 | The study design and the effect of treatment with a combination of 3BNC117 and 10-1074 on plasma viraemia in the study participants. a,

Schematic of the clinical trial design. The blue triangles indicate infusions of 3BNC117 and 10-1074 or placebo. F/U, follow-up; W, week. **b,** Plasma viraemia of the study participants. The participants in group 1 were randomized to receive either a combination of anti-HIV broadly neutralizing antibodies (bNAbs) 3BNC117 (30 mg kg⁻¹) and 10-1074 (30 mg kg⁻¹) ($n = 7$) or placebo ($n = 7$). ART was discontinued 3 days after receiving the first dose of bNAbs or placebo. Group 2 (open-label) consisted of 5 ART-naïve individuals with viraemic control. The blue triangles indicate the time of administration of the antibodies or placebo. The grey shaded boxes indicate the duration of ATI. The grey dotted horizontal lines indicate the limit of detection of the assay (40 copies of HIV RNA per ml). The white triangles indicate undetectable plasma viraemia (<40 copies of HIV RNA per ml) and the red triangles indicate detectable plasma viraemia (≥ 40

copies of HIV RNA per ml). Plasma antibody concentrations were determined using the TZM-bl assay. The dark blue and green circles indicate the plasma concentration of 3BNC117 and 10-1074, respectively. The x axis label (time (weeks)) applies to all of the plots in **b, c**. **c,** Kaplan–Meyer analysis of suppression of plasma viraemia after ATI in the study participants in group 1. Comparison of the proportion of the study participants remaining off ART during ATI in the bNAb versus placebo arm (left). The vertical dotted line indicates the virological end point. Right, the duration of plasma viraemia at below 200 copies of HIV RNA per ml after ATI was compared between the participants in the bNAb arm and the placebo arm. *P* values were determined using exact log-rank tests. **d,** Comparison of plasma viraemia at the time of ART reinitiation between the bNAb ($n = 6$) and placebo ($n = 6$) arms in the group 1 study participants. The grey bars represent the geometric mean values. The *P* value was determined using a two-sided Mann–Whitney *U*-test.

The sensitivity (80% inhibitory concentration (IC₈₀)) of replication-competent HIV isolates to 3BNC117 and 10-1074 was longitudinally monitored in the study participants before and after the infusions of bNAbs. At the baseline, 38% of the study participants in group 1 had resistant (IC₈₀ > 10 µg ml⁻¹) infectious HIV to either 3BNC117 (3 out of 13 participants, 23%), 10-1074 (3 out of 13 participants, 23%), or both bNAbs (1 out of 13 participants, 8%) (Fig. 2a). There was no evidence that antibody-resistant virus emerged over time for the participants (02, 05, 06, 08 and 13) in the bNAb arm of group 1 who maintained sustained virological suppression during ATI (Fig. 2a). Notably, participant 01, whose baseline virus was largely resistant to 3BNC117, started developing resistance to 10-1074 at week 16 after ATI. Moreover, the baseline virus of participant 14, whose plasma viraemia rebounded >40 copies per ml within 6 weeks after ATI, was highly resistant to both antibodies (Fig. 2a), although only one infectious isolate could be examined due to the extraordinarily low frequency of CD4⁺ T cells carrying replication-competent HIV. Three out of the five group 2 participants, whose baseline CD4⁺ T cells contained resistant infectious HIV to either bNAb, did not suppress their plasma viraemia and subsequently developed fully resistant virus to both 3BNC117 and 10-1074 (Fig. 2a). Notably, group 1 bNAb participant 02, who suppressed plasma viraemia for more than 43 weeks in the absence of ART, developed a marked resistance to 10-1074 (but not to 3BNC117) after plasma viral rebound, probably due to a longer half-life of 10-1074 compared with 3BNC117 that resulted in subtherapeutic concentrations in vivo²³ (Fig. 2b). After reinitiation of ART according to the protocol in participant 02, the proportion of CD4⁺ T cells carrying 10-1074-resistant replication-competent HIV gradually diminished over time, suggesting a natural decay of the viral reservoir carrying 10-1074-resistant virus in the absence of immunologic pressure²⁶. The precise half-life of each antibody could not be assessed in our study due to the unavailability of plasma immediately after each infusion. However, the overall pharmacokinetics observed in our study participants were similar to those of a previous study²³ (Fig. 2c). Collectively, our data suggest that bNAb therapy with 3BNC117 and 10-1074 does not lead to a precipitous accumulation of resistant HIV during long-term virological suppression, provided that antibody-resistant virus is not present at the baseline and serum antibody titres remain high.

The levels of CD4⁺ T cells carrying total HIV DNA, cell-associated HIV RNA, intact proviral DNA and replication-competent virus were longitudinally monitored in group 1 bNAb participants whose plasma viraemia remained suppressed >30 weeks after ATI (Fig. 3a). No statistical significance was reached when the levels of HIV reservoirs were compared between the two time points (weeks 0 and 24) (Fig. 3b). Furthermore, a comparison of the fold changes in the size of HIV reservoirs over time between the group 1 bNAb arm and a cohort of early-treated individuals who remained continuously on ART²⁸ showed no significant difference (Fig. 3c). A marked increase in the frequency of CD4⁺ T cells carrying total HIV DNA was observed in the group 1 placebo

participants after ATI (Extended Data Fig. 2a). Notably, a reduction (transient for participant S3) in the level of total HIV DNA in the CD4⁺ T cells was observed in group 2 participants whose plasma viraemia was suppressed after bNAb infusions (Extended Data Fig. 2b). These data suggest that the combination bNAbs did not have a significant effect on the persistent HIV reservoir in our study participants, although a long-term study involving a much larger cohort would be necessary to definitively address this question.

The effect of bNAbs on immune parameters

Throughout the bNAb infusion periods, the CD4⁺ T cell counts of all of the participants, including those in the placebo arm of group 1, remained stable (Extended Data Fig. 3a). Nonetheless, we considered whether immunologic abnormalities (such as inflammation and exhaustion)²⁹ occurred in study participants who received infusions of combination bNAbs and maintained extended periods of virological suppression. To this end, we used high-dimensional flow cytometry to longitudinally examine immune parameters in peripheral blood mononuclear cells of our study participants. The frequencies of TIGIT⁺, PD-1⁺, CD38⁺HLA-DR⁺ and subsets of CD8⁺ T cells remained unchanged over time in all of the groups (Extended Data Fig. 3b). Optimized *t*-distributed stochastic neighbour embedding using high-dimensional mapping of the 21-parameter flow cytometry data was conducted to monitor immune cells of the study participants over time (Extended Data Fig. 4a, b). A total of 15 distinct T cell clusters was identified by FlowSOM³⁰ analyses (Extended Data Fig. 4a–c). The levels of CD8⁺ T cell clusters remained stable over time in all of the groups (Extended Data Fig. 4d). Cytokines (IL-6, IL-8 and TNF), chemokines (MIP-1β and RANTES) and markers of immune activation (IL-2Rα, CD40, PD-L1, IP-10, C-reactive protein and d-dimer) measured in the plasma of the study participants between week 0 and week 24 all remained unchanged in all groups (Extended Data Fig. 5). Taken together, our data suggest that substantial immunologic abnormalities, as assessed by cellular phenotypes and plasma biomarkers, did not arise during prolonged ATI in study participants in whom the bNAb-mediated virological suppression was achieved.

Previous studies have demonstrated that passive transfer of bNAbs in SIV-infected animals^{24,31} and humans with HIV^{25,26}, including individuals whose plasma viraemia was controlled by bNAbs in the absence of ART²⁷, could potentially lead to enhanced antiviral immunity. In humans, HIV-Gag-specific CD4⁺ and CD8⁺ T cell responses peaked at week 6/7 and were no longer significant by week 18 (ref. ²⁷). We longitudinally examined HIV-specific CD8⁺ T cells in our study participants by performing intracellular cytokine staining after stimulation with a pool of overlapping HIV Gag peptides and molecular analyses of the HIV-specific CD8⁺ T cell receptor (TCR) repertoire. The level of polyfunctional (IFNγ⁺TNF⁺MIP-1β⁺) HIV-Gag-specific CD8⁺ T cells remained unchanged in group 1 bNAb and group 2 participants (Extended Data Fig. 6a). A modest increase in the frequency of HIV-specific CD8⁺ T cells

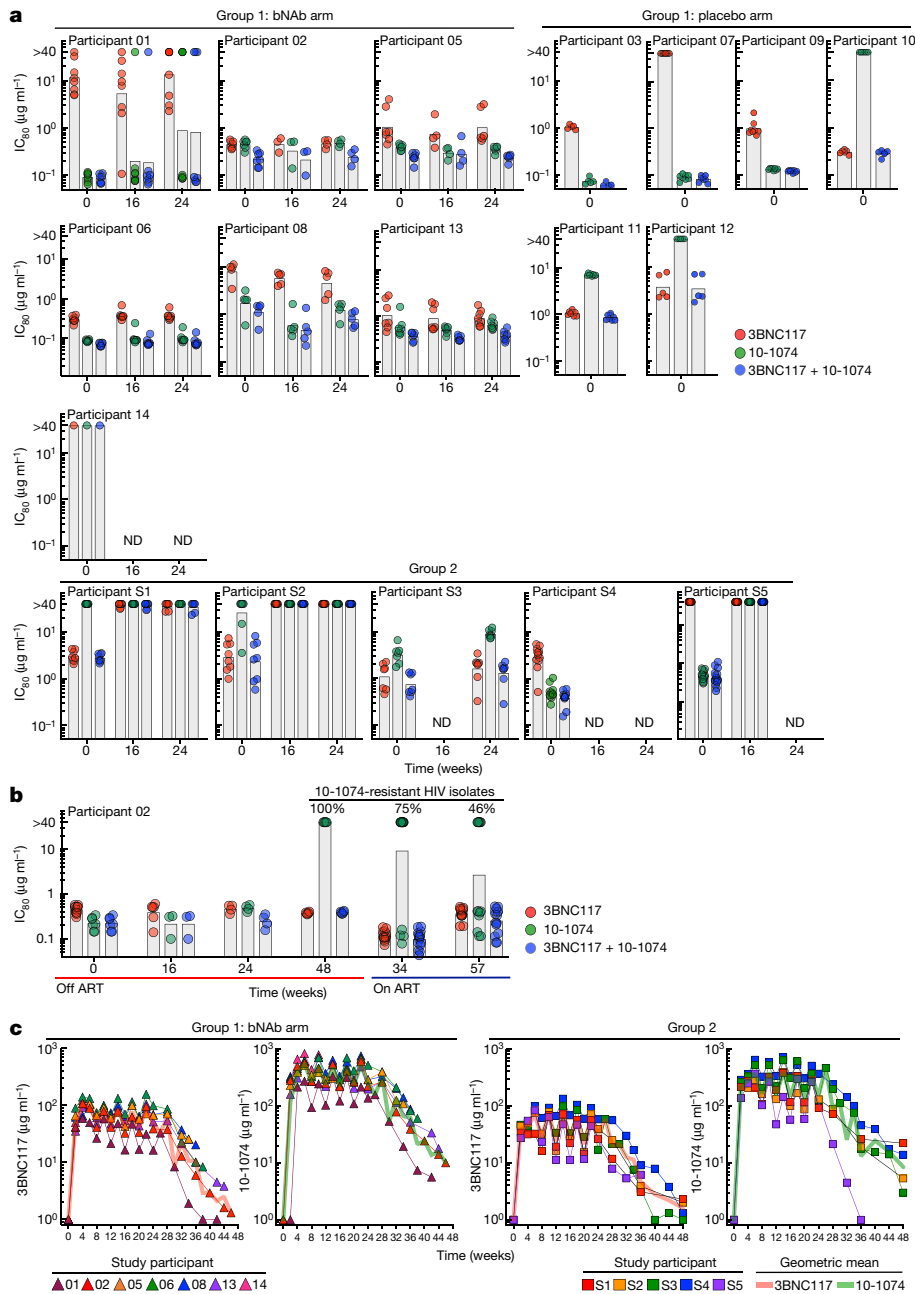


Fig. 2 | Sensitivity of replication-competent HIV to 3BNC117 and 10-1074 and pharmacokinetics. a, The IC₅₀ concentrations of 3BNC117 and 10-1074 against autologous, replication-competent viral isolates from the study participants. Near-clonal replication-competent HIV isolates were generated by co-culturing autologous CD4⁺ T cells with activated CD4⁺ T cells from healthy HIV-seronegative donors as described in the Methods. The IC₅₀ concentrations of 3BNC117 and 10-1074 against infectious HIV isolates were determined using the TZM-bl target cell neutralization assay. The grey bars indicate the geometric mean values. The x axis label (time (weeks)) applies to all

was observed over time in the group 1 placebo participants, probably due to the rising plasma viraemia after ATI (Extended Data Fig. 6a). To gain further insights into the effect of combination bNAbs on HIV-specific T cells at the molecular level, we conducted longitudinal deep-sequencing analysis of TCR genes using genomic DNA isolated from highly enriched CD8⁺ T cells. The average breadth of HIV-specific CD8⁺ TCR clonotypes remained stable in group 1 bNAb participants (Extended Data Fig. 6b). A modest increase, albeit statistically not significant ($P = 0.062$), in the depth of HIV-specific CD8⁺ TCR clonotypes

of the plots in **a, b**, The sensitivity of infectious HIV isolates derived from participant 02 to 3BNC117 and 10-1074. The IC₅₀ concentrations of 3BNC117 and 10-1074 against replication-competent viral isolates derived during ATI and after the reinitiation of ART were determined to examine the decay characteristics of antibody-resistant virus over time. **c**, Pharmacokinetics of 3BNC117 and 10-1074 in study participants. The plasma levels of 3BNC117 and 10-1074 were determined on the basis of a validated luciferase-based neutralization assay in TZM-bl cells. The red and green lines represent the geometric mean values of 3BNC117 and 10-1074, respectively.

was observed in these participants after passive transfer of the bNAbs. Notably, the breadth and depth of HIV-specific CD8⁺ TCR clonotypes in the group 1 placebo participants remained largely unchanged over time. There was a modest increase, albeit statistically not significant ($P = 0.062$), in the breadth of HIV-specific CD8⁺ TCR clonotypes in group 2 over time, possibly due to ongoing viral replication in 3 out of the 5 participants. To further investigate the changes in the TCR repertoires of the study participants, we compared the frequencies of the HIV-specific clonotypes at three different time points. For each group,

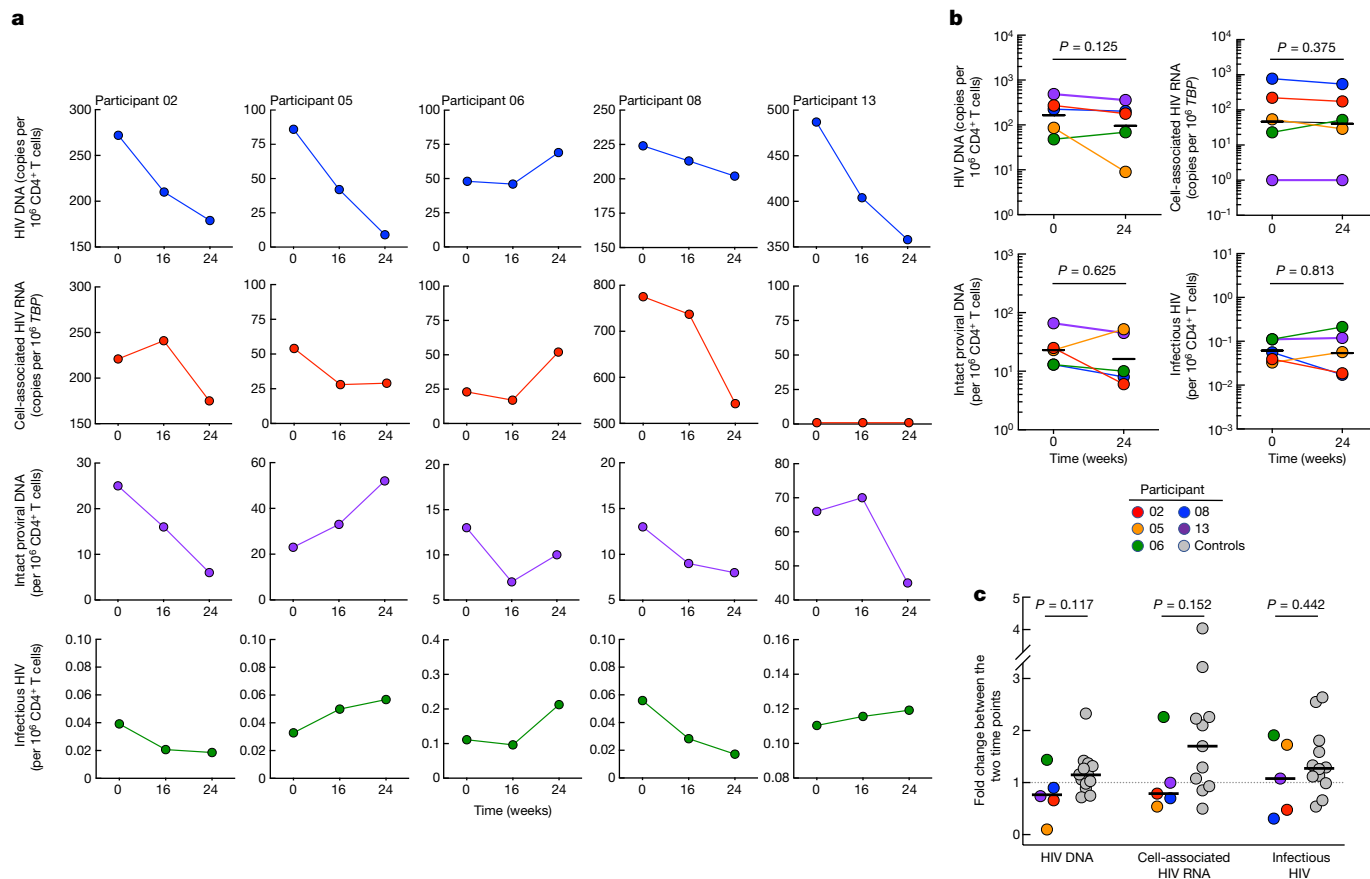


Fig. 3 | Dynamics of HIV reservoirs. a, Frequencies of CD4⁺ T cells carrying total HIV DNA, cell-associated HIV RNA, intact proviral DNA and replication-competent HIV are shown in five study participants in the bNAb arm of group 1 in whom sustained virological suppression was achieved after ATI. **b**, Dynamics of HIV reservoirs in the CD4⁺ T cells of group 1 bNAb study participants ($n = 5$) before and after multiple infusions of 3BNC117 and 10-1074. The black lines indicate the geometric mean values. Statistical significance was

tested using two-sided Wilcoxon matched-pairs signed-rank tests. **c**, Comparison of the fold changes in the size of HIV reservoirs over time between the bNAb arm ($n = 5$) and a control cohort of individuals with infection ($n = 13$) who initiated ART during the acute/early phase of infection and did not undergo therapeutic interventions or ATI. The black lines indicate the median values. P values were determined using two-sided Mann–Whitney U -tests.

the frequencies of the clonotypes present in the top 25 comparisons (Supplementary Table 3) that were ranked on the basis of statistical significance and the usage levels of the TRBV–TRBJ gene pairs in these clonotypes (Supplementary Table 4) were used to conduct principal component analysis. On the basis of the clonotype frequencies and gene usage levels, two reduced states for each TCR repertoire were computed. The variability of both repertoire states decreased at week 24 compared with at week 0 among the study participants in the bNAb arm of group 1, as illustrated by the smaller-sized ellipses over time (Extended Data Fig. 6b). A larger study involving multiple infusions of bNAbs and extended periods of follow-up will be necessary to confirm these findings.

Discussion

Despite decades of intensive research, the prospects of achieving an HIV cure as manifested by eradication of the virus remain elusive². A more realistic alternative to a cure may be through immune-based therapies aimed at achieving maximal virological suppression without the need for life-long and predominantly daily ART and without the need to eliminate the persistent HIV reservoir in individuals with infection^{32,33}. To date, one of the most promising and realistic approaches for accomplishing these outcomes is by infrequent passive infusions of combination HIV-specific bNAbs^{15–18}. Numerous HIV-specific bNAbs have been isolated in recent years^{16,17,34,35} and more than a dozen of them,

either as single or combination therapies, have been tested in humans for safety and therapeutic efficacy¹⁵. However, although certain bNAbs have been shown to be highly effective in neutralizing HIV in vitro by standardized assays involving large panels of HIV Env-pseudotyped viruses³⁵, it is becoming increasingly clear that durable and ART-free virological suppression will require a combination of two or more antibodies together with screening for bNAb resistance to the pre-existing virus in individuals with infection^{19,22}. The data obtained from our clinical trial, a randomized study involving participants in whom ART was initiated during the acute/early phase of infection with a long duration of follow-up, clearly demonstrated that complete and sustained virological suppression is achievable with intermittent administration of combination bNAbs. However, the combination bNAbs was ineffective in maintaining suppression of plasma viraemia in 2 out of 7 study participants in our small cohort in whom replication-competent HIV exhibited resistance to one or both antibodies at the baseline. This will potentially pose a substantial challenge for the treatment of individuals with HIV with bNAbs on a large scale. Nonetheless, our findings revealed several positive outcomes. Over the course of 24 weeks of virological suppression in the study participants who received the combination bNAbs, there were no significant immunologic or virological alterations, such as increases in immune activation and exhaustion or the size of HIV reservoirs. A recent study has demonstrated that combination bNAbs could further augment T-cell responses against HIV in individuals with infection while suppressing their plasma viraemia²⁷.

Although we did not observe any significant changes in the frequency of HIV-specific polyfunctional CD8⁺ T cells in our study, further studies with early and frequent time points²⁷, as well as detailed assessments of virus-specific proliferative and cytotoxic effector functions³⁶, may be needed to fully delineate the role of T cells in bNAb therapeutic agents. It is also plausible that the marked virological suppression mediated by the bNAbs in our study cohort (those who initiated ART during the acute/early phase of infection), combined with their relatively low HIV reservoir burden at baseline, may have prevented the formation of immune complexes¹⁸ and/or the residual levels of viral expression needed for the induction of robust antiviral T-cell responses^{33,37}. It also remains to be fully elucidated whether additional benefits of bNAbs, aside from their ability to neutralize HIV and maintain viral suppression in the absence of ART, can ultimately alter the course of infection (that is, long-term suppression of plasma viraemia in the absence of both bNAbs and ART) after clearance of the antibodies *in vivo*. Although a larger study involving multiple infusions of bNAbs and extended periods of follow-up will be necessary to address this question, our data strongly suggest that the virus will ultimately rebound after bNAb clearance after 24 weeks of bNAb therapy. In this regard, future trials may need to incorporate a prespecified ART initiation shortly after the last infusion of bNAbs to prevent the emergence of antibody-resistant virus in study participants.

One of the major confounding factors of this study is the small sample size and it is therefore essential to conduct a much larger study involving study participants in whom ART was initiated during the acute/early phase of infection to confirm our findings. Other major caveats of our study include the lack of lymphoid tissue analyses and the limited number of infusions (up to eight). Nonetheless, our findings offer clear evidence that combination bNAb therapy in individuals with HIV is safe and well tolerated and, for those with antibody-sensitive virus, offers marked virological suppression without any significant or unforeseen immunologic and virological anomalies. As the next generation of bNAbs with increased breadth and prolonged half-lives (>60 days)^{15,17,35} become available, there is a reason to believe that the infrequent administration (that is, twice a year) of such antibodies, possibly along with a long-acting injectable antiretroviral drug^{12–14}, could lead to ART-free HIV suppression for extended periods (years) in individuals with infection.

Online content

Any methods, additional references, Nature Research reporting summaries, source data, extended data, supplementary information, acknowledgements, peer review information; details of author contributions and competing interests; and statements of data and code availability are available at <https://doi.org/10.1038/s41586-022-04797-9>.

- Deeks, S. G., Lewin, S. R. & Havlir, D. V. The end of AIDS: HIV infection as a chronic disease. *Lancet* **382**, 1525–1533 (2013).
- Chun, T. W., Moir, S. & Fauci, A. S. HIV reservoirs as obstacles and opportunities for an HIV cure. *Nat. Immunol.* **16**, 584–589 (2015).
- Chun, T. W., Eisinger, R. W. & Fauci, A. S. Durable control of HIV infection in the absence of antiretroviral therapy: opportunities and obstacles. *JAMA* **322**, 27–28 (2019).
- Ndung'u, T., McCune, J. M. & Deeks, S. G. Why and where an HIV cure is needed and how it might be achieved. *Nature* **576**, 397–405 (2019).

- Cohn, L. B., Chomont, N. & Deeks, S. G. The biology of the HIV-1 latent reservoir and implications for cure strategies. *Cell Host Microbe* **27**, 519–530 (2020).
- Sengupta, S. & Siliciano, R. F. Targeting the latent reservoir for HIV-1. *Immunity* **48**, 872–895 (2018).
- Chun, T. W. et al. Presence of an inducible HIV-1 latent reservoir during highly active antiretroviral therapy. *Proc. Natl Acad. Sci. USA* **94**, 13193–13197 (1997).
- Finzi, D. et al. Identification of a reservoir for HIV-1 in patients on highly active antiretroviral therapy. *Science* **278**, 1295–1300 (1997).
- Wong, J. K. et al. Recovery of replication-competent HIV despite prolonged suppression of plasma viremia. *Science* **278**, 1291–1295 (1997).
- Margolis, D. M. et al. Curing HIV: seeking to target and clear persistent infection. *Cell* **181**, 189–206 (2020).
- Lewin, S. R. & Rasmussen, T. A. Kick and kill for HIV latency. *Lancet* **395**, 844–846 (2020).
- Swindells, S. et al. Long-acting cabotegravir and rilpivirine for maintenance of HIV-1 suppression. *N. Engl. J. Med.* **382**, 1112–1123 (2020).
- Orkin, C. et al. Long-acting cabotegravir and rilpivirine after oral induction for HIV-1 infection. *N. Engl. J. Med.* **382**, 1124–1135 (2020).
- Overton, E. T. et al. Long-acting cabotegravir and rilpivirine dosed every 2 months in adults with HIV-1 infection (ATLAS-2M), 48-week results: a randomised, multicentre, open-label, phase 3b, non-inferiority study. *Lancet* **396**, 1994–2005 (2021).
- Caskey, M., Klein, F. & Nussenzweig, M. C. Broadly neutralizing anti-HIV-1 monoclonal antibodies in the clinic. *Nat. Med.* **25**, 547–553 (2019).
- Haynes, B. F., Burton, D. R. & Mascola, J. R. Multiple roles for HIV broadly neutralizing antibodies. *Sci. Transl. Med.* **11**, eaaz2686 (2019).
- Gama, L. & Koup, R. A. New-generation high-potency and designer antibodies: role in HIV-1 treatment. *Annu. Rev. Med.* **69**, 409–419 (2018).
- Nishimura, Y. & Martin, M. A. Of mice, macaques, and men: broadly neutralizing antibody immunotherapy for HIV-1. *Cell Host Microbe* **22**, 207–216 (2017).
- Bar, K. J. et al. Effect of HIV antibody VRC01 on viral rebound after treatment interruption. *N. Engl. J. Med.* **375**, 2037–2050 (2016).
- Caskey, M. et al. Viraemia suppressed in HIV-1-infected humans by broadly neutralizing antibody 3BNC117. *Nature* **522**, 487–491 (2015).
- Caskey, M. et al. Antibody 10-1074 suppresses viremia in HIV-1-infected individuals. *Nat. Med.* **23**, 185–191 (2017).
- Scheid, J. F. et al. HIV-1 antibody 3BNC117 suppresses viral rebound in humans during treatment interruption. *Nature* **535**, 556–560 (2016).
- Mendoza, P. et al. Combination therapy with anti-HIV-1 antibodies maintains viral suppression. *Nature* **561**, 479–484 (2018).
- Nishimura, Y. et al. Early antibody therapy can induce long-lasting immunity to SHIV. *Nature* **543**, 559–563 (2017).
- Lu, C. L. et al. Enhanced clearance of HIV-1-infected cells by broadly neutralizing antibodies against HIV-1 *in vivo*. *Science* **352**, 1001–1004 (2016).
- Schoofs, T. et al. HIV-1 therapy with monoclonal antibody 3BNC117 elicits host immune responses against HIV-1. *Science* **352**, 997–1001 (2016).
- Niessl, J. et al. Combination anti-HIV-1 antibody therapy is associated with increased virus-specific T cell immunity. *Nat. Med.* **26**, 222–227 (2020).
- Sneller, M. C. et al. A randomized controlled safety/efficacy trial of therapeutic vaccination in HIV-infected individuals who initiated antiretroviral therapy early in infection. *Sci. Transl. Med.* **9**, eaan8848 (2017).
- Deeks, S. G. HIV infection, inflammation, immunosenescence, and aging. *Annu. Rev. Med.* **62**, 141–155 (2011).
- Van Gassen, S. et al. FlowSOM: using self-organizing maps for visualization and interpretation of cytometry data. *Cytometry A* **87**, 636–645 (2015).
- Nishimura, Y. et al. Immunotherapy during the acute SHIV infection of macaques confers long-term suppression of viremia. *J. Exp. Med.* **218**, e20201214 (2021).
- Barouch, D. H. & Deeks, S. G. Immunologic strategies for HIV-1 remission and eradication. *Science* **345**, 169–174 (2014).
- Collins, D. R., Gaiha, G. D. & Walker, B. D. CD8⁺ T cells in HIV control, cure and prevention. *Nat. Rev. Immunol.* **20**, 471–482 (2020).
- Kwong, P. D. & Mascola, J. R. HIV-1 vaccines based on antibody identification, B cell ontogeny, and epitope structure. *Immunity* **48**, 855–871 (2018).
- Sok, D. & Burton, D. R. Recent progress in broadly neutralizing antibodies to HIV. *Nat. Immunol.* **19**, 1179–1188 (2018).
- Collins, D. R. et al. Functional impairment of HIV-specific CD8⁺ T cells precedes aborted spontaneous control of viremia. *Immunity* **54**, 2372–2384 (2021).
- Migueles, S. A. & Connors, M. Success and failure of the cellular immune response against HIV-1. *Nat. Immunol.* **16**, 563–570 (2015).

Publisher's note Springer Nature remains neutral with regard to jurisdictional claims in published maps and institutional affiliations.

© This is a U.S. government work and not under copyright protection in the U.S.; foreign copyright protection may apply 2022

Methods

Study design, participants and procedures

The purpose of this clinical trial was to assess the safety, tolerability and virological efficacy of a combination of two bNABs 3BNC117 and 10-1074 in individuals with HIV. The study consisted of two components: a randomized, double-blind, placebo-controlled trial (group 1) and an open-label, single-arm trial (group 2). The study inclusion criteria for group 1 included start of ART within 12 weeks of being diagnosed with acute or early HIV infection, a CD4⁺ T cell count of >450 cells per µl at screening, continuous ART treatment with suppression of plasma viraemia below the limit of detection for ≥1 year and with general good health. The participants who had previously participated in an ATI study were not excluded. Acute infection was defined as plasma viraemia of greater than 2,000 copies of HIV RNA per ml with a negative HIV-1 enzyme immunoassay (EIA; criterion 1); a positive result from an HIV-1 EIA with a negative or indeterminate HIV-1 western blot that subsequently evolves to a confirmed positive result (criterion 2); or a negative result from an HIV-1 EIA within the past 4 months and plasma viraemia greater than 400,000 copies per ml in the setting of a potential exposure to HIV-1 (criterion 3). Early infection was defined as a negative result from an HIV-1 EIA within 6 months before a positive result from an HIV-1 EIA and confirmatory HIV-1 western blot (criterion 4); a negative result from a rapid HIV-1 test within 1 month before a positive result from an HIV-1 EIA and western blot (criterion 5); or the presence of low level of HIV antibodies as determined by having a positive EIA and western blot with a non-reactive detuned EIA according to a multi-assay testing algorithm for recent infection (criterion 6). The study inclusion criteria for group 2 included no ART within 24 months, plasma viraemia of 200–5,000 copies per ml, and at least two documented instances of plasma viraemia ≥200 copies per ml on at least two occasions in the 12 months before screening. The predetermined primary end point of the study was the rate of occurrence of grade 3 or higher adverse events or serious adverse events that were probably or definitely related to the study antibodies. Adverse events were determined according to the Division of AIDS Table for Grading the Severity of Adult and Pediatric Adverse Events, Version 2.1. The virological end points were the number of study participants who experienced plasma viral rebound after ATI and who met criteria to restart ART before study week 28 (group 1) or the number of study participants who achieved sustained suppression of plasma viraemia by study week 28 (group 2).

The study participants in group 1 were randomized to receive multiple (up to 8) infusions of 3BNC117 (30 mg kg⁻¹ body weight) and 10-1074 (30 mg kg⁻¹ body weight) or placebo during the 24-week period. One study participant (participant 05) whose regimen contained a non-nucleoside reverse transcriptase inhibitor (NNRTI) was switched to an integrase inhibitor-based regimen 2 weeks before ATI due to the long half-life of NNRTIs. The study participants in group 1 discontinued ART 3 days after the first infusion of 3BNC117 and 10-1074 or placebo. The protocol investigators and study participants in group 1 were blinded to treatment assignments for the duration of study. All of the study participants in group 2 received up to 8 infusions of 3BNC117 (30 mg kg⁻¹ body weight) and 10-1074 (30 mg kg⁻¹ body weight) during the 24-week period. The study participants received sequential 3BNC117 and 10-1074 intravenously according to their body weight over a 60 min period per antibody. Plasma viraemia and CD4⁺ T cell count were monitored every 2 weeks. Plasma viraemia was determined using the Abbott Real-Time HIV-1 assay with a detection limit of 40 copies of HIV RNA per ml. The study participants in group 1 discontinued antibody infusions or placebo and reinitiated ART if they met one of more of the following criteria during the ATI phase: (1) a confirmed >30% decline in baseline CD4⁺ T cell count; (2) an absolute CD4⁺ T cell count of <350 cells per µl; or (3) sustained plasma viraemia of >1,000 copies per ml for greater than 4 weeks. The study participants in group 2 discontinued antibody

infusions if their CD4⁺ T cells declined as specified above or they had an increase in baseline plasma viraemia of >0.5 log₁₀.

Blood and leukapheresed products were collected in accordance with protocols approved by the Institutional Review Board of the National Institute of Allergy and Infectious Diseases, National Institutes of Health (ClinicalTrials.gov ID: NCT03571204). All of the participants provided written informed consent.

Measurements of IC₈₀

Near-clonal replication-competent HIV isolates were derived from coculturing enriched CD4⁺ T cells of the study participants with CD8-depleted anti-CD3 stimulated peripheral blood mononuclear cells (PBMCs) from HIV-seronegative donors as described below. The concentration of each infectious viral isolate was initially determined by HIV p24 enzyme-linked immunosorbent assay (ELISA). Each isolate was titrated using a standard TZM-bl target cell assay. To determine the IC₈₀ concentrations of both antibodies against reservoir-derived replication-competent HIV over time, each viral isolate was incubated with serially diluted (40, 10, 2.5, 0.625, 0.156, 0.039 µg ml⁻¹ in duplicate) 3BNC117 and/or 10-1074 for 90 min followed by incubation with TZM-bl cells for 48 h. Cells were then lysed and substrate (Promega) was added to measure the luciferase activity (SparkControl, v.3.1, Tecan).

Pharmacokinetics of 3BNC117 and 10-1074

The levels of 3BNC117 and 10-1074 in the plasma of the study participants were longitudinally measured using a validated luciferase-based neutralization assay in TZM-bl cells as previously described³⁸. In brief, plasma samples were tested in duplicate using a primary 1:20 dilution with a fivefold titration series and tested against the HIV Env pseudotyped viruses Q461.e2 (3BNC117-sensitive/10-1074-resistant) and Du422.1 (10-1074-sensitive/3BNC117-resistant). Pseudotyped virus with murine leukaemia virus (MuLV) Env was used as a negative control. 3BNC117 and 10-1074 clinical drug products were used as positive controls and tested using a primary concentration of 10 µg ml⁻¹ with fivefold serial dilution series. Plasma concentrations (µg ml⁻¹) of 3BNC117 and 10-1074 were determined as follows: plasma 50% inhibitory dilution (ID₅₀) titre (dilution) × IC₅₀ titre (µg ml⁻¹) of 3BNC117 or 10-1074.

Quantification of HIV reservoirs

The frequency of CD4⁺ T cells carrying total HIV DNA was determined by droplet digital PCR as previously described³⁹. In brief, genomic DNA was isolated from highly enriched CD4⁺ T cells using the Puregene DNA extraction kit (Qiagen) and digested with restriction enzyme MscI (New England BioLabs). Subsequently, the digested genomic DNA was analysed using droplet digital PCR (QuantaSoft, v.1.7.4.0917, Bio-Rad) according to the manufacturer's instructions. The following PCR primers and probe were used for amplification of the 5' LTR region of HIV DNA: forward primer 5'-GRAACCCACTGCTTAAGCCTCAA-3' (nucleotides 506–528 in *HXB2*; GenBank: K03455.1), reverse primer 5'-TGTTCCGGGCGCCACTGCTAGAGA-3' (nucleotides 648–626) and probe 5'-6FAM-AGTAGTGTGTGCCCGTCTGTT-IABkFQ-3' (nucleotides 552–572). The following PCR primers and probe were used for amplification of the housekeeping gene *RPP30*: forward primer 5'-GATTTGGACCTGCGAGCG-3' (nucleotides 29–46; GenBank: NM_001104546.2), reverse primer 5'-GCGGCTGTCTCCACAAGT-3' (nucleotides 90–73) and probe 5'-HEX-TTCTGACCTGAAGGCTCTGCGC-IABkFQ-3' (nucleotides 49–70). Copy numbers of HIV DNA were normalized per 1 × 10⁶ CD4⁺ T cells.

The level of CD4⁺ T-cell-associated HIV RNA was determined by PCR with reverse transcription (RT-PCR). Total RNA was isolated from highly enriched CD4⁺ T cells using the RNeasy Mini kit (Qiagen), followed by synthesis of complementary DNA (cDNA) using the qScript XLT cDNA Master Mix (Quanta Biosciences) according to the manufacturer's instructions. cDNA was analysed using droplet digital PCR (Bio-Rad Laboratories) using the following primers: HIV-specific

primers HIV-US-F (5'-TCTCTAGCAGTGGCGCCCGAACA-3', nucleotides 626–648), HIV-US-R (5'-TCTCCTTCTAGCCTCCGCTAGTC-3', nucleotides 786–764) and HIV-US-probe (5'-6FAM-CAAGCCGAGTCTGCGTTCGAGAG-IABkFQ-3', nucleotides 705–683); and TATA-box-binding protein (*TBP*; housekeeping gene)-specific primers TBP-F (5'-CACGAACCACGGCACTGATT-3', nucleotides 863–882; GenBank: NM_003194.5) and TBP-R (5'-TTTCTTGTGCCAGTCTG GAC-3', nucleotides 951–930) and TBP-probe (5'-HEX-TGTGCACAGGA GCCAAGAGTGAAGA/3-IABkFQ-3', nucleotides 902–926). Copy numbers of cell-associated HIV RNA were normalized per 1×10^6 copies of *TBP*.

The frequency of CD4⁺ T cells carrying intact HIV proviruses was determined using the Intact Proviral DNA Assay (IPDA) as previously described⁴⁰.

The level of CD4⁺ T cells carrying replication-competent HIV was determined by quantitative co-culture assay using serially diluted and replicates of 5×10^6 CD4⁺ T cells as previously described³⁹. Highly enriched CD4⁺ T cells were incubated with anti-CD3 antibodies and irradiated PBMCs from healthy HIV-negative donors. After incubation for 1 day, 1×10^6 CD8-depleted and anti-CD3-stimulated PBMCs from HIV-negative donors were added to each well, followed by periodic removal of cell suspensions and replenishment with fresh medium containing IL-2. Subsequently, HIV p24 ELISA was performed on the culture supernatants to identify wells containing replication-competent HIV. The infectious units per million cells from quantitative coculture assays were determined as previously described⁴¹.

Phenotypic characterization of immune cells using flow cytometry

Cryopreserved PBMCs were thawed, washed and stained with the viability reagent Zombie NIR (BioLegend, 423106) and fluorophore-conjugated antibodies in Brilliant Stain Buffer Plus (BD, 566385). Flow cytometry data were acquired on the Cytek Aurora cytometer using the SpectroFlo Software (Cytek Biosciences) and analysed using FlowJo v.10.7.1 and the OMIQ platform (<https://www.omiq.ai/>).

High-dimensional data analysis of flow cytometry data

Optimized *t*-distributed stochastic neighbour embedding (opt-SNE) and FlowSOM analyses were conducted using OMIQ software (<https://www.omiq.ai/>). Opt-SNE analysis was performed using equal sampling of 100,000 CD3⁺ T cells from each FCS file, with 1,000 iterations, a perplexity of 30 and a theta of 0.5. The following immune markers were used to generate opt-SNE maps: CD4, CD8, CD45RA, CCR7, CD27, CD28, CD38, HLA-DR, CD226, TIGIT, PD-1, 2B4, CD160, CTLA-4, CD96, OX40, CXCR5, ICOS and 4-1BB. The resulting opt-SNE maps were used for the FlowSOM algorithm. The self-organizing map was generated using hierarchical consensus clustering and 15 meta-clusters were identified. The heat map displaying column-scaled z-scores of mean fluorescence intensity for individual FlowSOM clusters was generated using OMIQ platform.

Intracellular cytokine staining assay

The frequency of virus-specific CD8⁺ T cells was assessed by incubating PBMCs with a pool of HIV-1 consensus B Gag overlapping peptides (NIH AIDS Reagent Program) with brefeldin A (Sigma-Aldrich) for 6 h at 37 °C. Unstimulated cells were used as a negative control for background subtraction. Cells were stained with Zombie NIR (BioLegend, 423106) and antibodies to immune markers (Supplementary Table 5). Cells were then fixed with 1× lysing solution (BD Biosciences) and permeabilized with 1× permeabilization solution 2 (BD Biosciences). After washing, cells were stained with the antibodies to the intracellular cytokines and chemokines (Supplementary Table 5 and Supplementary Fig. 1). Data were acquired on the Cytek Aurora cytometer using the SpectroFlo Software (Cytek Biosciences) and analysed using FlowJo v.10.7.1.

TCR repertoire analysis

Complementarity determining regions (CDR) 3 of TCR β-chains present in highly enriched CD8⁺ T cells of the study participants were sequenced in a high-throughput manner using the immunoSEQ assay^{42,43} after amplification of the extracted DNA in a bias-controlled multiplex PCR. The resulting CDR3 sequences were collapsed and filtered to quantify the absolute abundance and frequency of each unique TCR β region with immunoSEQ Analyzer (Adaptive Biotechnologies)⁴⁴. TCR repertoire statistics, including gene usage (the fraction of clonotypes in which a given TRBV or TRBJ gene is present), were computed using Immunarch⁴⁵. TCR sequencing data are available online (<https://clients.adaptivebiotech.com/login>; login: chun-review@adaptivebiotech.com, password: chun2021review). HIV-specific breadth and depth were computed using the HIV-specific CDR3 sequences previously reported in the literature from four databases, namely the immune epitope database (IEDB)⁴⁶, VDjdb⁴⁷, McPAS-TCR⁴⁸ and the Pan immune repertoire database (PIRD)⁴⁹. The reported breadth values represent the fraction of clonotypes in each repertoire that are HIV-specific, whereas depth calculations take the abundance of each clonotype into account, such that each HIV-specific clonotype affects the overall HIV-specific depth (per sample) with a magnitude proportional to its abundance.

Measurements of biomarkers in plasma

Levels of biomarkers in plasma were determined using the ELLA platform (Simple Plex Runner, v.3.7.2.0, ProteinSimple) according to the manufacturer's instructions.

Statistical analysis

P values for the virological end points (group 1) were determined using exact log-rank tests. Sensitivity analyses were performed to handle the two study participants (11 and 14) who reinitiated ART before meeting the restart criteria. Two independent analyses, with and without censoring the data from the above study participants, generated the same *P* values.

P values for paired and unpaired comparisons were computed using Wilcoxon signed-rank tests and Mann–Whitney *U*-tests, respectively, using Prism v.9.1 (GraphPad). *P* values computed in the TCR repertoire analysis were determined using Wilcoxon signed rank tests (paired) and Mann–Whitney *U*-tests (unpaired) using the R package ggpubr⁵⁰. The factoMineR⁵¹ package in R was used to perform PCA with the TCR repertoire data.

Reporting summary

Further information on research design is available in the Nature Research Reporting Summary linked to this paper.

Data availability

TCR sequencing data are available online (<https://clients.adaptivebiotech.com/login>; login: chun-review@adaptivebiotech.com, password: chun2021review). The HIV-specific CDR3 sequences were downloaded from the following four databases: the immune epitope database (IEDB; <http://www.iedb.org/>), VDjdb (<https://vdjdb.cdr3.net>), McPAS-TCR (<http://friedmanlab.weizmann.ac.il/McPAS-TCR/>) and the Pan Immune Repertoire Database (PIRD; <https://db.cngb.org/pird/>).

Code availability

The R scripts that were used in the data analysis have been deposited at GitHub (<https://github.com/cihangenome/comboination-antibodies-HIV>). The following R packages were used: factoextra (v.1.0.7), FactoMineR (v.2.4), reshape (v.0.8.8), reshape2 (v.1.4.4), writexl (v.1.4.0), gdata (v.2.18.0), psych (v.2.1.9), car (v.3.0-11), carData (v.3.0-4), corrr (v.0.4.3), lubridate (v.1.8.0), readxl (v.1.3.1),

forcats (v.0.5.1), stringr (v.1.4.0), purrr (v.0.3.4), readr (v.2.0.2), tidyr (v.1.1.4), tibble (v.3.1.5), tidyverse (v.1.3.1), ggpubr (v.0.4.0), immunarch (v.0.6.6), patchwork (v.1.1.1), data.table (v.1.14.2), dtplyr (v.1.1.0), dplyr (v.1.0.7) and ggplot2 (v.3.3.5).

38. Sarzotti-Kelsoe, M. et al. Optimization and validation of the TZM-bl assay for standardized assessments of neutralizing antibodies against HIV-1. *J. Immunol. Methods* **409**, 131–146 (2014).
39. Clarridge, K. E. et al. Effect of analytical treatment interruption and reinitiation of antiretroviral therapy on HIV reservoirs and immunologic parameters in infected individuals. *PLoS Pathog.* **14**, e1006792 (2018).
40. Bruner, K. M. et al. A quantitative approach for measuring the reservoir of latent HIV-1 proviruses. *Nature* **566**, 120–125 (2019).
41. Myers, L. E., McQuay, L. J. & Hollinger, F. B. Dilution assay statistics. *J. Clin. Microbiol.* **32**, 732–739 (1994).
42. Robins, H. S. et al. Comprehensive assessment of T-cell receptor β -chain diversity in $\alpha\beta$ T cells. *Blood* **114**, 4099–4107 (2009).
43. Carlson, C. S. et al. Using synthetic templates to design an unbiased multiplex PCR assay. *Nat. Commun.* **4**, 2680 (2013).
44. Snyder, T. M. et al. Magnitude and dynamics of the T-cell response to SARS-CoV-2 infection at both individual and population levels. Preprint at *MedRxiv* <https://doi.org/10.1101/2020.07.31.20165647> (2020).
45. ImmunoMind Team. immunarch: an R package for painless bioinformatics analysis of T-cell and B-cell immune repertoires (version 0.6.7) (Zenodo, 2019).
46. Vita, R. et al. The immune epitope database (IEDB): 2018 update. *Nucleic Acids Res.* **47**, D339–D343 (2019).
47. Shugay, M. et al. VDJdb: a curated database of T-cell receptor sequences with known antigen specificity. *Nucleic Acids Res.* **46**, D419–D427 (2018).
48. Tickotsky, N., Sagiv, T., Prilusky, J., Shifrut, E. & Friedman, N. McPAS-TCR: a manually curated catalogue of pathology-associated T cell receptor sequences. *Bioinformatics* **33**, 2924–2929 (2017).
49. Zhang, W. et al. PIRD: pan immune repertoire database. *Bioinformatics* **36**, 897–903 (2020).

50. Kassambara, A. ggpubr: 'ggplot2' based publication ready plots. R package version 0.1.7 (2018).
51. Lê, S., Josse, J. & Husson, F. FactoMineR: an R package for multivariate analysis. *J. Stat. Softw.* **25**, 1–18 (2008).

Acknowledgements We thank the study volunteers for their participation in this study; D. Asmuth, J. Mascola and S. Read for their guidance; and the NIAID HIV Outpatient Clinic staff for their assistance in the execution of this study. This work was supported by the Intramural Research Program of the National Institute of Allergy and Infectious Diseases, National Institutes of Health.

Author contributions M.C.S. and T.-W.C. designed the clinical trial and research. J.B., J.S.J., V.S., B.D.K., E.J.W., R.F.S. M.S.S., S.M. and T.-W.C. performed experiments. J.B. and C.O. performed bioinformatic analysis. M.C.S., K.G., J.T., G.M., E.B., C.K. and T.-W.C. contributed to recruitment of study participants. M.C. and M.C.N. provided study drugs. M.C.S., J.B., M.A.P., C.O., M.S.S., S.M. and T.-W.C. analysed data. M.C.S., A.S.F., S.M. and T.-W.C. wrote the manuscript.

Competing interests M.C.N. is listed as an inventor for patents on 3BNC117 (PTC/US2012/038400) and 10-1074 (PTC/US2013/065696); 3BNC117 and 10-1074 are licensed to Gilead Sciences by Rockefeller University from which M.C.N. has received payments. M.C.N. is a member of the Scientific Advisory Boards of Celldex Therapeutics, Walking Fish Therapeutics and Frontier Biotechnologies. M.C.N. had no control over the direction and ultimately the reporting of the clinical portion of the research while holding their financial interests. The other authors declare no competing interests.

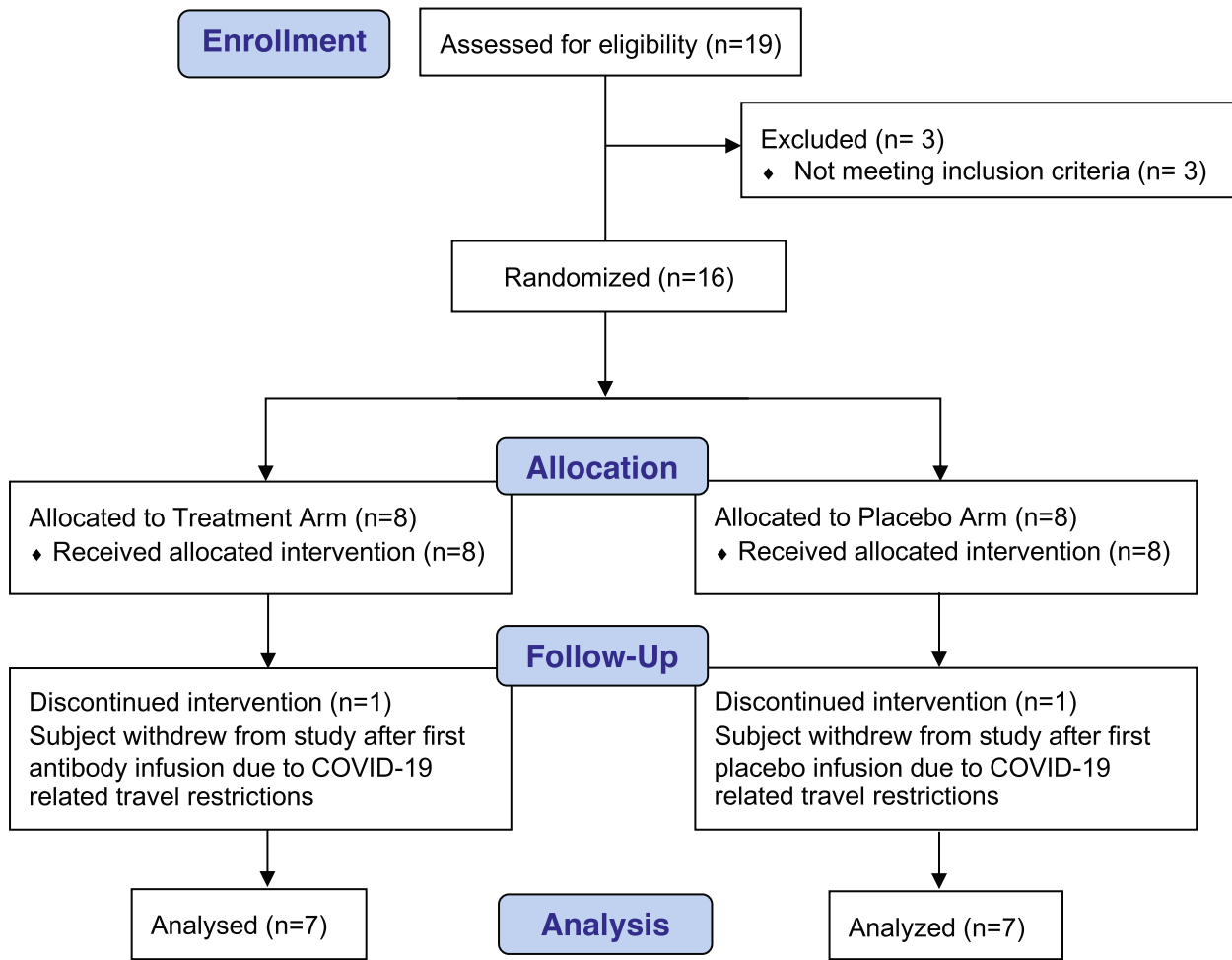
Additional information

Supplementary information The online version contains supplementary material available at <https://doi.org/10.1038/s41586-022-04797-9>.

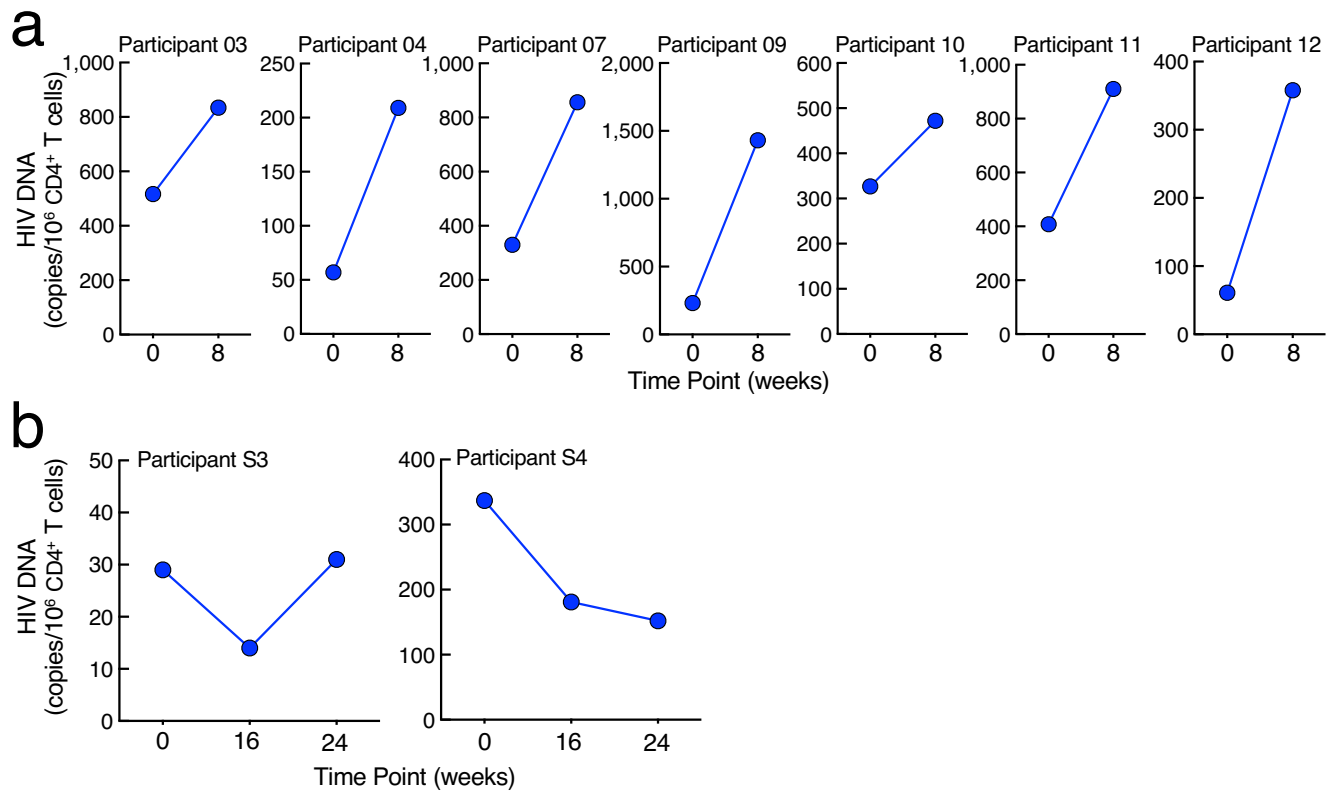
Correspondence and requests for materials should be addressed to Tae-Wook Chun.

Peer review information Nature thanks Lu Zheng and the other, anonymous, reviewer(s) for their contribution to the peer review of this work.

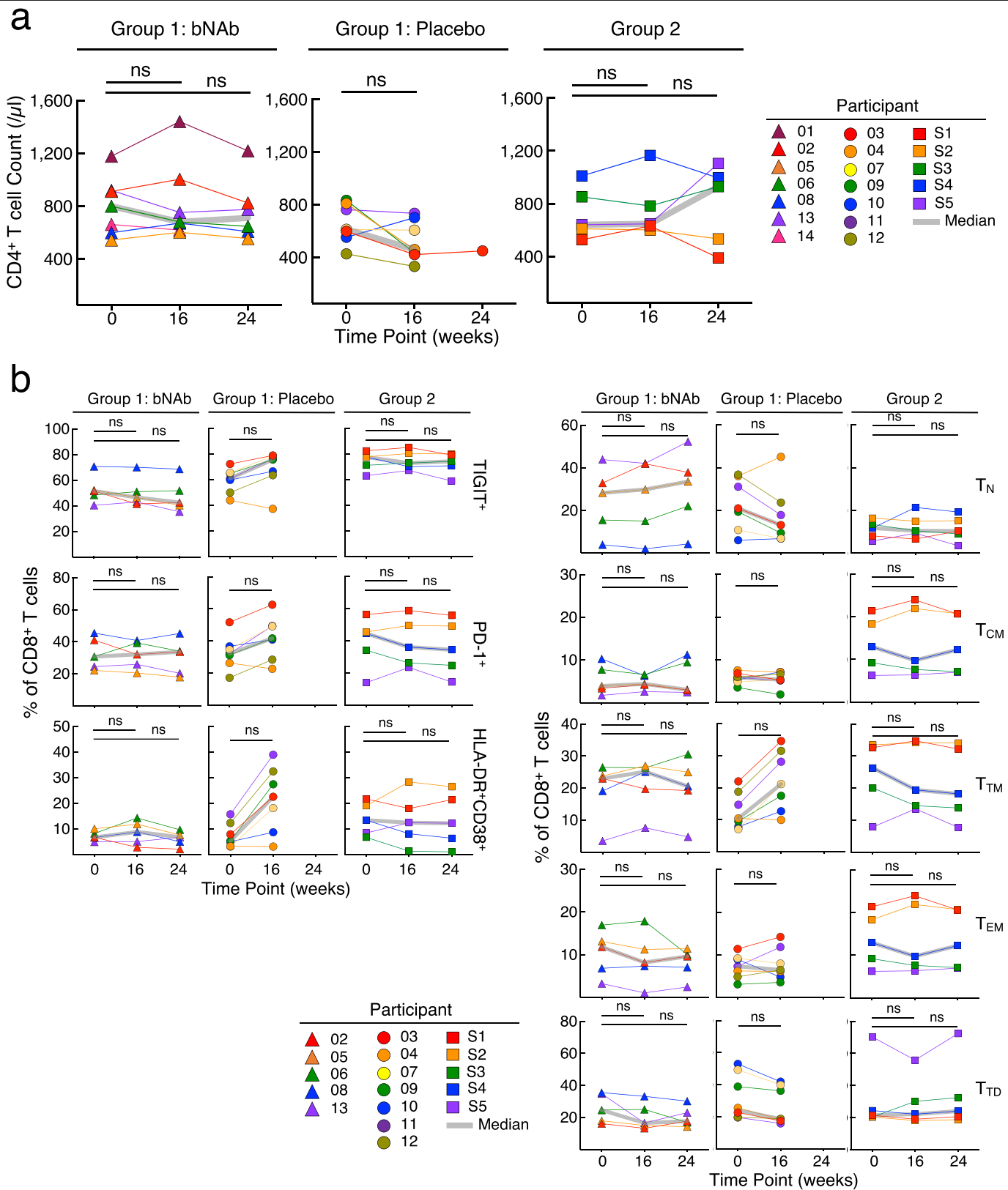
Reprints and permissions information is available at <http://www.nature.com/reprints>.



Extended Data Fig.1 | Consolidated Standards of Reporting Trials (CONSORT) flow diagram for the trial. CONSORT diagram shows the study enrolment of 14 participants who underwent randomization to the bNAb or placebo groups.

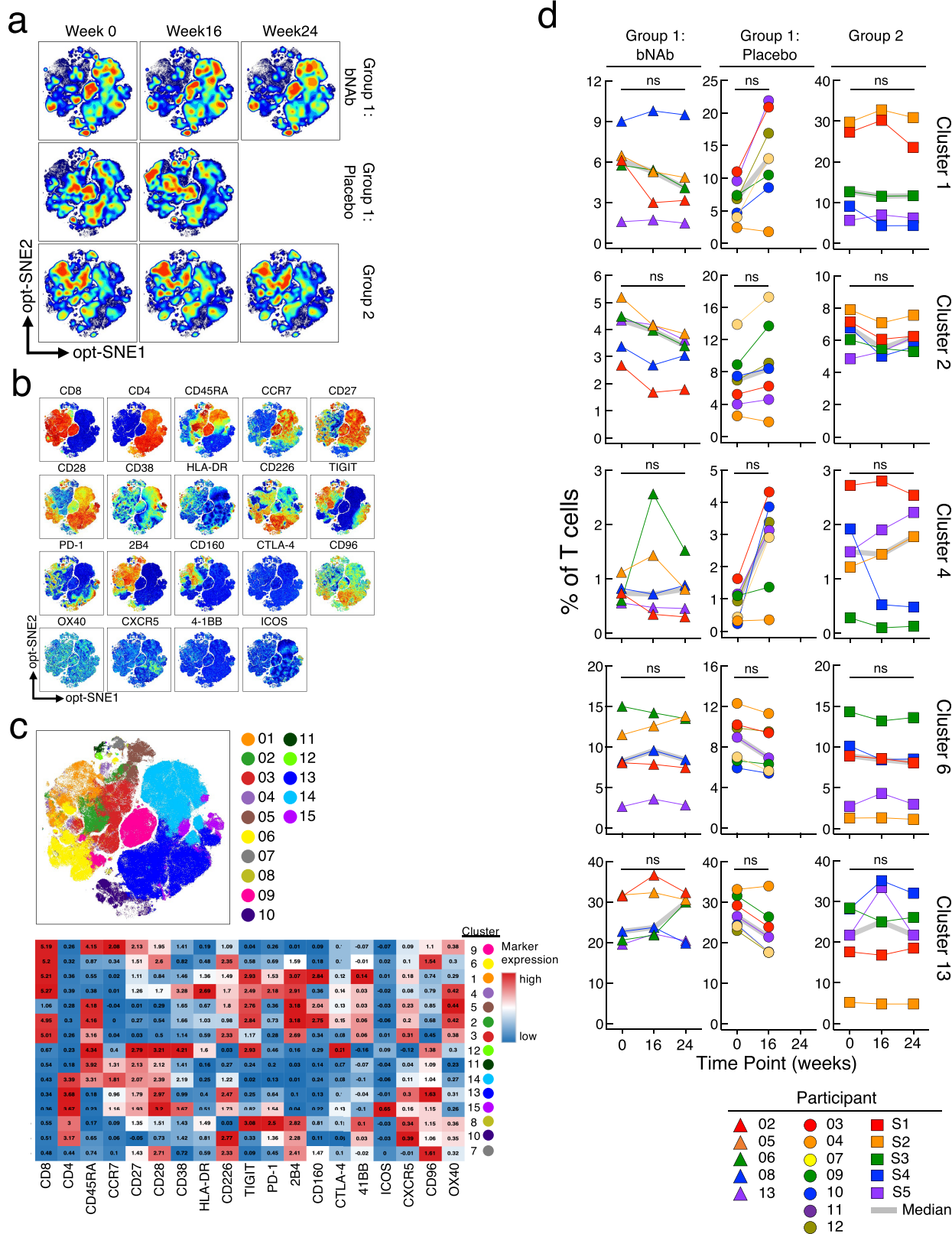


Extended Data Fig. 2 | Dynamics of HIV reservoirs. a. Frequencies of CD4⁺ T cells carrying total HIV DNA in study participants in the placebo arm of Group 1. **b.** Frequencies of CD4⁺ T cells carrying total HIV DNA in study participants in the Group 2 in whom plasma viraemia was suppressed by the combination bNAbs.



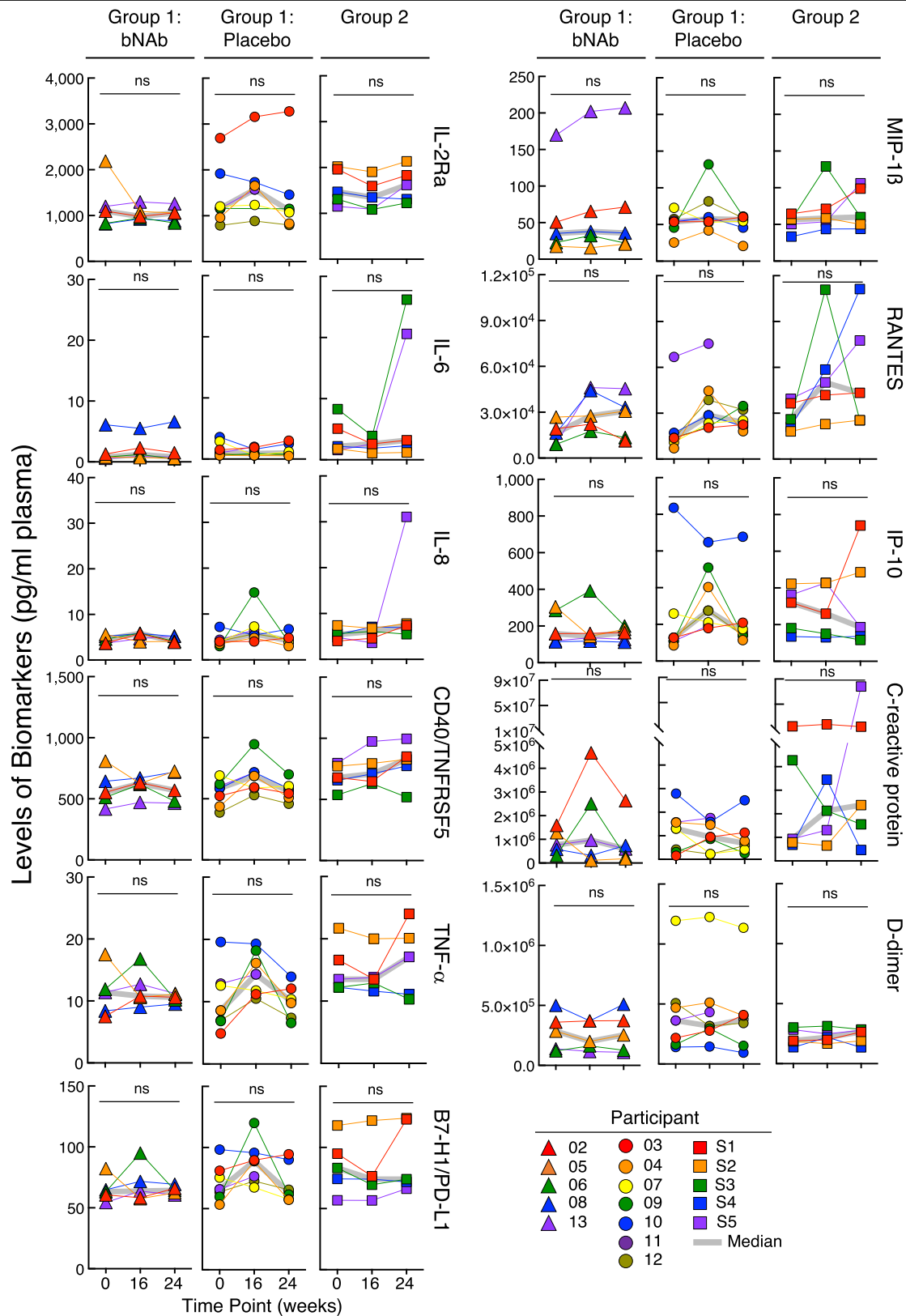
Extended Data Fig. 3 | Longitudinal measurements of CD4⁺ T cell counts and phenotypic analyses of CD8⁺ T cells. **a.** Levels of CD4⁺ T cell counts of the bNAb (n = 7) and placebo (n = 7) arms of Group 1 and Group 2 (n = 5) study participants are shown. **b.** Frequencies of the activation/exhaustion markers TIGIT, PD-1, CD38 and HLA-DR (left) and T cell subsets (T_N, naive; T_{CM}, central memory; T_{TM}, transitional memory; T_{EM}, effector memory; T_{TD}, terminally

differentiated) on CD8⁺ T cells of the bNAb (n = 5) and placebo (n = 7) arms of Group 1 and Group 2 (n = 5) study participants are shown. The grey lines indicate median values. *P* values were determined using the two-sided Wilcoxon matched-pairs signed rank test and were adjusted for multiple testing. ns, not significant.



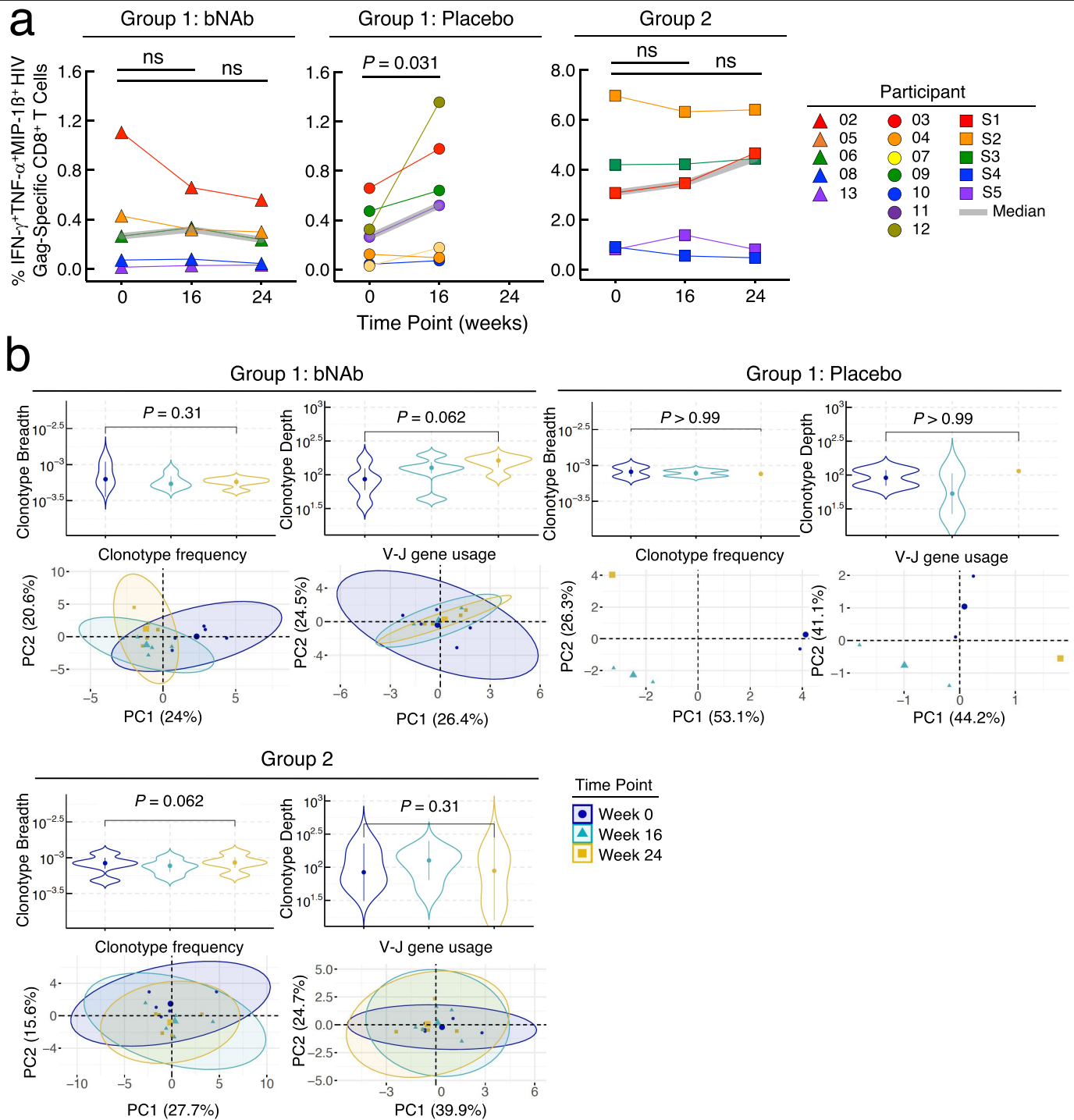
Extended Data Fig. 4 | Phenotypic analysis of T cells. Longitudinal high-dimensional flow cytometric analyses of PBMCs of study participants. **a.** Global opt-SNE plots of CD3⁺ T cells of combined data from each group of study participants. **b.** Opt-SNE visualization of expression of the indicated markers are shown. **c.** Opt-SNE map of T cell clusters identified by FlowSOM clustering. Each number indicates a distinct cluster. Heatmap shows the level of

expression (MFI) within individual clusters. **d.** Comparison of frequencies of T cells expressing markers associated with indicated clusters in the bNAb (n = 5) and placebo (n = 7) arms of Group 1 and Group 2 (n = 5) study participants are shown. P values were determined using the two-sided Wilcoxon matched-pairs signed rank test and were adjusted for multiple testing. ns, not significant.



Extended Data Fig. 5 | Levels of biomarkers in the plasma of the bNAb (n = 5) and placebo (n = 7) arms of Group 1 and Group 2 (n = 5) study participants over time. The grey lines indicate median values. *P* values were

determined using the two-sided Wilcoxon matched-pairs signed rank test and were adjusted for multiple testing. ns, not significant.



Extended Data Fig. 6 | Analysis of HIV-specific CD8⁺ T cells. Frequencies of HIV Gag-specific CD8⁺ T cells and dynamics of CD8⁺ T cell receptor (TCR) repertoire. **a.** Frequencies of polyfunctional (IFN- γ +TNF- α +MIP-1 β) HIV Gag-specific CD8⁺ T cells in the bNAb (n = 5) and placebo (n = 7) arms of Group 1 and Group 2 (n = 5) study participants are shown. The grey lines indicate median values. *P* values were determined using the two-sided Wilcoxon matched-pairs signed rank test. **b.** Changes in the HIV-specific breadth and depth of CD8⁺ T cells of study participants are shown (upper panels). Highly enriched CD8⁺ T cells were obtained using a bead-based purification method. The analysis includes 35 CD8⁺ T cell-derived genomic DNA samples from 12 study participants (15 samples from 5 participants in the bNAb arm of Group 1, 5 samples from 2 participants in the placebo arm of Group 1, and 15 samples from 5 participants in Group 2). Violin plots show the Gaussian kernel probability density of the breadth/depth values over time. The median values and interquartile ranges of the time point-specific distribution are shown as circles

and vertical lines, respectively. Principal component analysis (PCA) of the changes in the TCR repertoire characteristics is shown (lower panels). Each ellipse shows the 95% confidence interval in the PCA space and the center of each ellipse is indicated by larger sized symbols that represent specific time points. Lower left panels depict PCA results with the frequencies of the HIV-specific clonotypes ranked among the top 25 with respect to their *P* values associated with the pairwise comparisons between the three time points. Lower right panels depict PCA results with the gene usage profiles derived from the TRBV-TRBJ gene pairs in the above clonotypes. Principal component (PC) 1 and PC2 represent a lower-dimensional representation of the input data consisting of the frequencies of the HIV-specific clonotypes (lower left panel) and the usage levels of the TRBV-TRBJ gene pairs (lower right panel) for each patient group. *P* values were determined using the two-sided Wilcoxon signed-rank test.

Reporting Summary

Nature Portfolio wishes to improve the reproducibility of the work that we publish. This form provides structure for consistency and transparency in reporting. For further information on Nature Portfolio policies, see our [Editorial Policies](#) and the [Editorial Policy Checklist](#).

Statistics

For all statistical analyses, confirm that the following items are present in the figure legend, table legend, main text, or Methods section.

n/a Confirmed

- The exact sample size (n) for each experimental group/condition, given as a discrete number and unit of measurement
- A statement on whether measurements were taken from distinct samples or whether the same sample was measured repeatedly
- The statistical test(s) used AND whether they are one- or two-sided
Only common tests should be described solely by name; describe more complex techniques in the Methods section.
- A description of all covariates tested
- A description of any assumptions or corrections, such as tests of normality and adjustment for multiple comparisons
- A full description of the statistical parameters including central tendency (e.g. means) or other basic estimates (e.g. regression coefficient) AND variation (e.g. standard deviation) or associated estimates of uncertainty (e.g. confidence intervals)
- For null hypothesis testing, the test statistic (e.g. F , t , r) with confidence intervals, effect sizes, degrees of freedom and P value noted
Give P values as exact values whenever suitable.
- For Bayesian analysis, information on the choice of priors and Markov chain Monte Carlo settings
- For hierarchical and complex designs, identification of the appropriate level for tests and full reporting of outcomes
- Estimates of effect sizes (e.g. Cohen's d , Pearson's r), indicating how they were calculated

Our web collection on [statistics for biologists](#) contains articles on many of the points above.

Software and code

Policy information about [availability of computer code](#)

Data collection

Data analysis

For manuscripts utilizing custom algorithms or software that are central to the research but not yet described in published literature, software must be made available to editors and reviewers. We strongly encourage code deposition in a community repository (e.g. GitHub). See the Nature Portfolio [guidelines for submitting code & software](#) for further information.

Data

Policy information about [availability of data](#)

All manuscripts must include a [data availability statement](#). This statement should provide the following information, where applicable:

- Accession codes, unique identifiers, or web links for publicly available datasets
- A description of any restrictions on data availability
- For clinical datasets or third party data, please ensure that the statement adheres to our [policy](#)

TCR sequencing data are available at <https://clients.adaptivebiotech.com/login> (login: chun-review@adaptivebiotech.com and password: chun2021review). The

HIV-specific CDR3 sequences were downloaded from the following four databases: the immune epitope database (IEDB: <http://www.iedb.org/>), VDJDdb (<https://vdjdb.cdr3.net>), McPAS-TCR (<http://friedmanlab.weizmann.ac.il/McPAS-TCR/>), and the Pan immune repertoire database (PIRD: <https://db.cngb.org/pird/>).

Field-specific reporting

Please select the one below that is the best fit for your research. If you are not sure, read the appropriate sections before making your selection.

Life sciences Behavioural & social sciences Ecological, evolutionary & environmental sciences

For a reference copy of the document with all sections, see [nature.com/documents/nr-reporting-summary-flat.pdf](https://www.nature.com/documents/nr-reporting-summary-flat.pdf)

Life sciences study design

All studies must disclose on these points even when the disclosure is negative.

Sample size

The randomized controlled portion of the study had a planned enrollment of 30 study participants. However, the study was prematurely halted in February 2020 due to safety concerns associated with treatment interruption of ART in the setting of the COVID-19 pandemic.

The primary safety outcome is the occurrence of grade 3 or higher AEs. An exact 95% confidence interval for the probability of AEs will be computed using the Clopper-Pearson method. The primary efficacy outcome is rebound of plasma viremia requiring a restart of ART. An exact 95% confidence interval will be computed for the rebound probability using the Clopper-Pearson method. Changes from baseline in continuous measurements will be analyzed using paired t-tests or, if data are skewed, the Wilcoxon signed rank statistic. In terms of safety, a sample size of 30 subjects provides a 95.8% chance of observing an AE of probability 10% or greater. Table 1 shows the chance of observing at least one AE of given probability.

Table 1. Chance of AE of Given Probability

	Probability					
Row 1	0.025	0.050	0.075	0.100	0.125	0.150
Row 2	0.532	0.785	0.904	0.958	0.982	0.992

The second row is the probability of observing at least one AE of probability given in the first row for the 30 subjects receiving 3BNC117 plus 10-1074.

Group 1 Efficacy Endpoint

Sample size justification is based on data from a recently completed NIAID therapeutic vaccine study of early treated subjects (ClinicalTrials.gov Identifier: NCT01859325). In the Placebo arm of the therapeutic vaccine study, 80% of subjects would have met the criteria to restart ART prior to study week 32. Table 2 shows power for ART restart probabilities between 0.20 and 0.30 in the 3BNC117 plus 10-1074 arm. Power is approximately 87% and 80% for ART restart probabilities of 0.20 and 0.24 in the 3BNC117 plus 10-1074 arm.

Table 2. Power shown in row 2 for different ART restart probabilities in the 3BNC117 plus 10-1074 arm (row 1). The restart probability in the placebo arm is assumed to be 0.80.

Restart Prob. bNAb arm	0.20	0.22	0.24	0.26	0.28	0.30
Power	0.872	0.840	0.804	0.765	0.724	0.680

Data exclusions

No data were excluded.

Replication

Plasma viremia was determined using an automated system and reagents. CD4 and CD8 T cell counts were determined by CLIA certified laboratories. All viral reservoir measurements were done in triplicate or quadruplicate, with consistent values among individual replicates. All longitudinal flow cytometry data were generated using highly standardized methods. All other experiments were performed once at each time point.

Randomization

Study participants of the Group 1 were randomly allocated into bNAb or Placebo arm.

Blinding

The investigators were blinded to group allocation until the data collection from all study participants was terminated.

Reporting for specific materials, systems and methods

We require information from authors about some types of materials, experimental systems and methods used in many studies. Here, indicate whether each material, system or method listed is relevant to your study. If you are not sure if a list item applies to your research, read the appropriate section before selecting a response.

Materials & experimental systems

n/a	Involved in the study
<input type="checkbox"/>	<input checked="" type="checkbox"/> Antibodies
<input type="checkbox"/>	<input checked="" type="checkbox"/> Eukaryotic cell lines
<input checked="" type="checkbox"/>	<input type="checkbox"/> Palaeontology and archaeology
<input checked="" type="checkbox"/>	<input type="checkbox"/> Animals and other organisms
<input type="checkbox"/>	<input checked="" type="checkbox"/> Human research participants
<input type="checkbox"/>	<input checked="" type="checkbox"/> Clinical data
<input checked="" type="checkbox"/>	<input type="checkbox"/> Dual use research of concern

Methods

n/a	Involved in the study
<input checked="" type="checkbox"/>	<input type="checkbox"/> ChIP-seq
<input type="checkbox"/>	<input checked="" type="checkbox"/> Flow cytometry
<input checked="" type="checkbox"/>	<input type="checkbox"/> MRI-based neuroimaging

Antibodies

Antibodies used

1. CD3 BUV805, SK7, BD Biosciences, catalog #612893
2. CD4 BUV395, M-T477, BD Biosciences, catalog #742738
3. CD8 BUV737, SK1, BD Biosciences, catalog #612755
4. CD45RA PerCP-Cy5.5, HI100, BD Biosciences, catalog #563429
5. CCR7 V450, 150503, BD Biosciences, catalog #560864
6. CD27 Alexa Fluor 700, M-T271, BD Biosciences, catalog #560611
7. CD28 BUV496, CD28.2, BD Biosciences, catalog #741168
8. CD38 BB515, HIT2, BD Biosciences, catalog #564498
9. CD226 BV480, DX11, BD Biosciences, catalog #746405
10. PD-1 PE-Cy7, EH12.1, BD Biosciences, catalog #561272
11. CD160 Alexa Fluor 647, BY55, BD Biosciences, catalog #562362
12. CTLA-4 PE-Cy5, BNI3, BD Biosciences, catalog #561717
13. CD96 BV711, 6F9, BD Biosciences, catalog #563174
14. OX40 BV786, ACT35, BD Biosciences, catalog #743285
15. CXCR5 BV510, RF8B2, BD Biosciences, catalog #563105
16. ICOS BV421, DX29, BD Biosciences, catalog #562901
17. HLA-DR Super Bright 436, LN3, eBioscience catalog #62-9956
18. TIGIT PE-eFluor 610, MBSA43, eBioscience catalog #61-9500
19. 2B4 PE, C1.7, eBioscience catalog #12-5838
20. 2B4 BV605, C1.7, BioLegend catalog #329536
21. 4-1BB APC, 4B4-1, BioLegend catalog #309810
22. TNF- α BV650, MAb11, BD Biosciences, catalog #563418
23. IFN- γ APC, B27, BD Biosciences, catalog #554702
24. MIP-1b PE, D21-1351, BD Biosciences, catalog #550078

Validation

1. CD3 BUV805; Reactivity: Human (QC testing, BD Biosciences); Application: Flow cytometry (Routinely Tested, BD Biosciences)
2. CD4 BUV395; Reactivity: Human (Tested in Development, BD Biosciences); Application: Flow cytometry (Qualified, BD Biosciences)
3. CD8 BUV737; Reactivity: Human (QC testing, BD Biosciences), Rhesus, Cynomolgus, Baboon (Tested in Development); Application: Flow cytometry (Routinely Tested, BD Biosciences)
4. CD45RA PerCP-Cy5.5; Reactivity: Human (QC testing, BD Biosciences); Application: Flow cytometry (Routinely Tested, BD Biosciences)
5. CCR7 V450; Reactivity: Human (QC testing, BD Biosciences); Application: Flow cytometry (Routinely Tested, BD Biosciences)
6. CD27 Alexa Fluor 700; Reactivity: Human (QC testing, BD Biosciences), Rhesus, Cynomolgus, Baboon (Tested in Development); Application: Flow cytometry (Routinely Tested, BD Biosciences)
7. CD28 BUV496; Reactivity: Human (Tested in Development, BD Biosciences); Application: Flow cytometry (Qualified, BD Biosciences)
8. CD38 BB515; Reactivity: Human (QC testing, BD Biosciences); Application: Flow cytometry (Routinely Tested, BD Biosciences)
9. CD226 BV480; Reactivity: Human (Tested in Development, BD Biosciences); Application: Flow cytometry (Qualified, BD Biosciences)
10. PD-1 PE-Cy7; Reactivity: Human (QC testing, BD Biosciences); Application: Flow cytometry (Routinely Tested, BD Biosciences)
11. CD160 Alexa Fluor 647; Reactivity: Human (QC testing, BD Biosciences); Application: Flow cytometry (Routinely Tested, BD Biosciences)
12. CTLA-4 PE-Cy5; Reactivity: Human (QC testing, BD Biosciences), Rhesus, Cynomolgus, Baboon (Tested in Development); Application: Flow cytometry (Routinely Tested, BD Biosciences), Intracellular staining Flow cytometry (Tested During Development)
13. CD96 BV711; Reactivity: Human (QC testing, BD Biosciences); Application: Flow cytometry (Routinely Tested, BD Biosciences)
14. OX40 BV786; Reactivity: Human (Tested in Development, BD Biosciences); Application: Flow cytometry (Qualified, BD Biosciences)
15. CXCR5 BV510; Reactivity: Human (QC testing, BD Biosciences); Application: Flow cytometry (Routinely Tested, BD Biosciences)
16. ICOS BV421; Reactivity: Human (QC testing, BD Biosciences); Application: Flow cytometry (Routinely Tested, BD Biosciences)
17. HLA-DR Super Bright 436; Reactivity: Human (eBioscience); Application: Flow cytometry (eBioscience)
18. TIGIT PE-eFluor 610; Reactivity: Human (eBioscience); Application: Flow cytometry (eBioscience)
19. 2B4 PE; Reactivity: Human (eBioscience); Application: Flow cytometry (eBioscience)
20. 2B4 BV605; Reactivity: Human (BioLegend); Application: Flow cytometry (Quality tested, BioLegend)
21. 4-1BB APC; Reactivity: Human (BioLegend), Cross-Reactivity: Chimpanzee, Baboon, Cynomolgus, Rhesus; Application: Flow cytometry (Quality tested, BioLegend)
22. TNF- α BV650; Reactivity: Human (QC testing, BD Biosciences), Rhesus, Cynomolgus, Baboon (Tested in Development); Application: Intracellular staining Flow cytometry (Routinely Tested, BD Biosciences)
23. IFN- γ APC; Reactivity: Human (QC testing, BD Biosciences), Rhesus, Cynomolgus, Baboon (Tested in Development); Application: Intracellular staining Flow cytometry (Routinely Tested, BD Biosciences)

Eukaryotic cell lines

Policy information about [cell lines](#)

Cell line source(s)	TZM-bl cells (ARP-8129): HIV Reagent Program (https://www.hivreagentprogram.org/Catalog/cellBanks/ARP-8129.aspx)
Authentication	The above cell line was not authenticated.
Mycoplasma contamination	TZM-bl cell line (ARP-8129) is negative for bacteria, Mycoplasma and fungi.
Commonly misidentified lines (See ICLAC register)	No commonly misidentified lines were used in this study.

Human research participants

Policy information about [studies involving human research participants](#)

Population characteristics	<p>The study consisted of two components: a randomized, double-blind, placebo-controlled trial (Group 1) and an open label, single arm trial (Group 2). Study inclusion criteria for Group 1 included institution of ART within 12 weeks of being diagnosed with primary HIV infection, CD4+ T cell count >450 cells/μl at screening, and continuous ART treatment with suppression of plasma viremia below the limit of detection for ≥1 year. HIV-infected participants were eligible if they were in general good health and had initiated ART within 90 days of being diagnosed with acute or early HIV infection. Acute infection was defined as a plasma viremia greater than 2,000 copies of HIV RNA/ml with a negative HIV-1 enzyme immunoassay (EIA; criterion 1), a positive result from an HIV-1 EIA with a negative or indeterminate HIV-1 Western blot that subsequently evolves to a confirmed positive result (criterion 2), or negative result from an HIV-1 EIA within the past 4 months and plasma viremia greater than 400,000 copies/ml in the setting of a potential exposure to HIV-1 (criterion 3). Early infection was defined as a negative result from an HIV-1 EIA within 6 months before a positive result from an HIV-1 EIA and confirmatory HIV-1 Western blot (criterion 4), a negative result from a rapid HIV-1 test within 1 month before a positive result from an HIV-1 EIA and Western blot (criterion 5), or the presence of low level of HIV antibodies as determined by having a positive EIA and Western blot with a nonreactive detuned EIA according to a multi-assay testing algorithm for recent infection (criterion 6). Study inclusion criteria for Group 2 included no ART within 24 months, plasma viremia between 200-5,000 copies/ml, and at least two documented plasma viremia ≥200 copies/ml on at least two occasions in the 12 months prior to screening.</p> <p>Clinical profiles of Study Participants</p> <p>Group Age Gender Race HIV Risk</p> <p>Group 1: bNAb</p> <p>01 45 Male White MSM 02 40 Male Black MSM 05 27 Male Asian MSM 06 40 Male White MSM 08 57 Male White MSM 13 38 Male White/Hispanic MSM 14 39 Male White MSM</p> <p>Group 1: Placebo</p> <p>03 32 Male White MSM 04 33 Male White MSM 07 56 Male White MSM 09 41 Male White MSM 10 52 Male White MSM 11 34 Male White/Hispanic MSM 12 29 Male Asian MSM</p> <p>Group 2</p> <p>S1 35 Male White MSM S2 44 Male Multiple Race MSM S3 40 Male White MSM S4 52 Male White MSM S5 52 Male Black MSM</p>
Recruitment	Study participants were enrolled at the Clinical Center, National Institute of Allergy and Infectious Diseases, National Institutes of Health, Bethesda, MD 20892, USA.
Ethics oversight	Institutional review board of National Institute of Allergy and Infectious Diseases, National Institutes of Health, Bethesda, MD 20892, USA.

Note that full information on the approval of the study protocol must also be provided in the manuscript.

Clinical data

Policy information about [clinical studies](#)

All manuscripts should comply with the ICMJE [guidelines for publication of clinical research](#) and a completed [CONSORT checklist](#) must be included with all submissions.

Clinical trial registration	NCT03571204
Study protocol	https://clinicaltrials.gov/ct2/show/NCT03571204 Protocol documents are available upon request.
Data collection	Data were collected in the National Institutes of Health Clinical Center (National Institute of Allergy and Infectious Diseases (NIAID)), between September 2018 and March 2021.
Outcomes	The predetermined primary endpoint of the study was the rate of occurrence of grade 3 or higher AE or SAEs which were probably or definitely related to the study antibodies. AEs were determined according to the Division of AIDS Table for Grading the Severity of Adult and Pediatric Adverse Events, Version 2.1. The virologic endpoints were the number of study participants who experienced plasma viral rebound following ATI and who met criteria to restart ART before study week 28 (Group 1) or the number of study participants who achieved sustained suppression of plasma viremia by study week 28 (Group 2).

Flow Cytometry

Plots

Confirm that:

- The axis labels state the marker and fluorochrome used (e.g. CD4-FITC).
- The axis scales are clearly visible. Include numbers along axes only for bottom left plot of group (a 'group' is an analysis of identical markers).
- All plots are contour plots with outliers or pseudocolor plots.
- A numerical value for number of cells or percentage (with statistics) is provided.

Methodology

Sample preparation	Cryopreserved PBMCs were thawed, washed, and stained, or thawed, washed, rested, stimulated, fixed, permeabilized and stained according to the demands on each experiment (as described in the Methods section).
Instrument	Cytek Aurora (2019)
Software	Data were acquired using the SpectroFlo Software (Cytek Biosciences) and analyzed using FlowJo version 10.7.1, and OMIQ platform (www.Omiq.ai)
Cell population abundance	We collected on average 200,000 CD3+ lymphocytes for each sample. FMO controls and mock-treated cells were used as controls.
Gating strategy	The cells were gated as follows: Lymphocyte population identified by FSC-A/SSC-A, followed by single cells (FSC-H/FSC-A), followed by the dead cell exclusion using Zombie NIR stain. Next, the T lymphocytes were identified as CD3+ (CD3/SSC-A gate), followed by gating of CD4+ and CD8+ T cells (CD4/CD8 plot). CD4+ and CD8+ T cells were further analyzed separately, identification of T-cell subsets were as follows: Naive (CD45RA+CCR7+CD27+), Terminally differentiated (TTD; CD45RA+CCR7-CD27-), Central memory (TCM; CD45RA-CCR7+CD27+), Transitional memory (TTM; CD45RA-CCR7-CD27+), Effector memory (TEM; CD45RA-CCR7-CD27-). CD8+ T cells were also analyzed for activation (HLA-DR, CD38) and exhaustion/inhibition (TIGIT, CD226, PD-1, 2B4, CD160, CTLA-4) markers. Expression of intracellular cytokines IFNg, TNFa and MIP-1b was identified by individual gating within the CD8+ T cells population, and single-, double- and triple-positive cells were identified by Boolean gating.

- Tick this box to confirm that a figure exemplifying the gating strategy is provided in the Supplementary Information.